

1 **Responses to Referee #1's comments**

2 We are grateful to the reviewers for their valuable and helpful comments on our manuscript  
3 "Reaction of SO<sub>3</sub> with H<sub>2</sub>SO<sub>4</sub> and Its Implication for Aerosol Particle Formation in the Gas Phase  
4 and at the Air-Water Interface" (MS No.: **egusphere-2023-2009**). We have revised the manuscript  
5 carefully according to reviewers' comments. The point-to-point responses to the Referee #1's  
6 comments are summarized below:

7

8 **Referee Comments:**

9 Rui Wang and co-authors have used computational methods to study the formation and clustering  
10 of H<sub>2</sub>S<sub>2</sub>O<sub>7</sub>-known (depending on the source) as either disulfuric acid, pyrosulfuric acid, or oleum.  
11 The technical methods used in the study are broadly appropriate, and the context (atmospheric new-  
12 particle formation involving different sulfur compounds) is certainly relevant and broadly  
13 interesting. The study is thus without doubt publishable. However, I have some critical notes about  
14 the interpretation of the results, and their atmospheric implications (which I believe to be overstated,  
15 at least in the context of Earth's lower atmosphere).

16 **Response:** We would like to thank the reviewer for the positive and valuable comments, and we  
17 have revised our manuscript accordingly.

18 **Major issues**

19 **Comment 1.**

20 As shown by Torrent-Sucarrat (JACS 2012; cited in the present study), the SO<sub>3</sub> + H<sub>2</sub>SO<sub>4</sub> reaction in  
21 the presence of water can also lead directly to H<sub>2</sub>SO<sub>4</sub> + H<sub>2</sub>SO<sub>4</sub> (instead of H<sub>2</sub>S<sub>2</sub>O<sub>7</sub>). Given that  
22 H<sub>2</sub>SO<sub>4</sub> is pretty much always hydrated, water is - as the authors themselves argue here - essentially  
23 always present in the reaction system, at least in the lower troposphere. Thus, an explicit  
24 consideration of the competition between the two channels would be warranted - however this seems  
25 to be missing in the study. The authors should try to estimate what percentage of SO<sub>3</sub> + H<sub>2</sub>SO<sub>4</sub>  
26 collisions, in different hydration environments, we can expect to yield (at least transiently, see below)  
27 H<sub>2</sub>S<sub>2</sub>O<sub>7</sub>, as compared to H<sub>2</sub>SO<sub>4</sub> + H<sub>2</sub>SO<sub>4</sub>? (Note that this question should be asked on top of the  
28 question that they DO address, i.e. "what fraction of SO<sub>3</sub> will collide with H<sub>2</sub>SO<sub>4</sub> as opposed to H<sub>2</sub>O,  
29 or H<sub>2</sub>O\*X, where X is any other catalyst for the SO<sub>3</sub> hydration reaction. As per the authors own

1 calculation in their Table S6, already this percentage is very small-despite their neglect of many  
2 other known candidates for X.)

3 **Response:** Thanks for your valuable comments. According to the reviewer's suggestion, the  
4 schematic potential energy surface of the H<sub>2</sub>SO<sub>4</sub> formation from the SO<sub>3</sub> + H<sub>2</sub>SO<sub>4</sub> reaction with  
5 H<sub>2</sub>O has been added in Fig. 1, while the corresponding effective rate constants have been listed in  
6 Table 1. Then, the competition between H<sub>2</sub>SO<sub>4</sub> and H<sub>2</sub>S<sub>2</sub>O<sub>7</sub> formations from the SO<sub>3</sub> + H<sub>2</sub>SO<sub>4</sub>  
7 reaction with H<sub>2</sub>O have been discussed. The corresponding major revision has been made as follows.

8 (a) The SO<sub>3</sub> + H<sub>2</sub>SO<sub>4</sub> reaction with H<sub>2</sub>O can produce two distinct products, labeled (i) H<sub>2</sub>S<sub>2</sub>O<sub>7</sub>  
9 (DSA, Channel DSA\_WM) and (ii) H<sub>2</sub>SO<sub>4</sub> (SA, Channel SA\_SA). A single water molecule in (i)  
10 acts as a catalyst, while it plays as a reactant in (ii). So, based on the H<sub>2</sub>S<sub>2</sub>O<sub>7</sub> formation from the  
11 SO<sub>3</sub> + H<sub>2</sub>SO<sub>4</sub> reaction with H<sub>2</sub>O, the schematic potential energy surface for the H<sub>2</sub>SO<sub>4</sub> formation  
12 from the SO<sub>3</sub> + H<sub>2</sub>SO<sub>4</sub> reaction with H<sub>2</sub>O is also involved in Fig. 1. In Lines 18-21 Page 8 of the  
13 revised manuscript, the corresponding discussion has been reorganized as “The SO<sub>3</sub> + H<sub>2</sub>SO<sub>4</sub>  
14 reaction with H<sub>2</sub>O produced two distinct products, labeled (i) H<sub>2</sub>S<sub>2</sub>O<sub>7</sub> (DSA, Channel DSA\_WM)  
15 and (ii) H<sub>2</sub>SO<sub>4</sub> (SA, Channel SA\_SA). A single water molecule in (i) acted as a catalyst, while it  
16 played as a reactant in (ii). The schematic potential energy surface for the SO<sub>3</sub> + H<sub>2</sub>SO<sub>4</sub> reaction  
17 with H<sub>2</sub>O was shown in Fig. 1.”

18 (b) Similar with the H<sub>2</sub>S<sub>2</sub>O<sub>7</sub> formation from the SO<sub>3</sub> + H<sub>2</sub>SO<sub>4</sub> reaction with H<sub>2</sub>O (Fig. 1 (b),  
19 Channel DSA\_WM), the H<sub>2</sub>SO<sub>4</sub> formation from the SO<sub>3</sub> + H<sub>2</sub>SO<sub>4</sub> reaction with H<sub>2</sub>O (Fig. 1 (c),  
20 Channel SA\_SA) can be considered as a sequential bimolecular process. In other words, Channel  
21 SA\_SA occurs via the collision between SO<sub>3</sub> (or H<sub>2</sub>SO<sub>4</sub>) and H<sub>2</sub>O to form dimer (SO<sub>3</sub>···H<sub>2</sub>O and  
22 H<sub>2</sub>SO<sub>4</sub>···H<sub>2</sub>O) first, and then the dimer encounters with the third reactant H<sub>2</sub>SO<sub>4</sub> or SO<sub>3</sub>. However,  
23 the SO<sub>3</sub>···H<sub>2</sub>O + H<sub>2</sub>SO<sub>4</sub> reaction in Channel SA\_SA can be neglected as its effective rate constant  
24 is smaller by 1.02-3.05 times than the corresponding value in the H<sub>2</sub>SO<sub>4</sub>···H<sub>2</sub>O + SO<sub>3</sub> reaction.  
25 Therefore, we only consider the H<sub>2</sub>SO<sub>4</sub>···H<sub>2</sub>O + SO<sub>3</sub> bimolecular reaction in Channel SA\_SA. In  
26 Lines 21-29 Page 8 to lines 1-17 Page 9 of the revised manuscript, two sequential bimolecular  
27 processes, H<sub>2</sub>SO<sub>4</sub>···H<sub>2</sub>O + SO<sub>3</sub> and SO<sub>3</sub>···H<sub>2</sub>O + H<sub>2</sub>SO<sub>4</sub>, have been considered, which has been  
28 reorganized as “As the probability of simultaneous collision (Pérez-Ríos et al., 2014; Elm et al.,  
29 2013) of three molecules of SO<sub>3</sub>, SA and H<sub>2</sub>O is quite low under realistic conditions, both Channel  
30 DSA\_WM and Channel SA\_SA can be considered as a sequential bimolecular process. In other

1 words, both Channel DSA\_WM and Channel SA\_SA occur via the collision between SO<sub>3</sub> (or H<sub>2</sub>SO<sub>4</sub>)  
2 and H<sub>2</sub>O to form dimer (SO<sub>3</sub>···H<sub>2</sub>O and H<sub>2</sub>SO<sub>4</sub>···H<sub>2</sub>O) first, and then the dimer encounters with the  
3 third reactant H<sub>2</sub>SO<sub>4</sub> or SO<sub>3</sub>. The computed Gibbs free energies of dimer complexes SO<sub>3</sub>···H<sub>2</sub>O and  
4 H<sub>2</sub>SO<sub>4</sub>···H<sub>2</sub>O were respectively 0.8 kcal·mol<sup>-1</sup> and -1.9 kcal·mol<sup>-1</sup>, which were respectively  
5 consistent with the previous values (the range from -0.2 to 0.62 kcal·mol<sup>-1</sup> for SO<sub>3</sub>···H<sub>2</sub>O complex  
6 (Bandyopadhyay et al., 2017; Long et al., 2012) and the range from -1.82 to -2.63 kcal·mol<sup>-1</sup> for  
7 H<sub>2</sub>SO<sub>4</sub>···H<sub>2</sub>O complex (Long et al., 2013b; Tan et al., 2018)). The Gibbs free energy of H<sub>2</sub>SO<sub>4</sub>···H<sub>2</sub>O  
8 was lower by 2.7 kcal·mol<sup>-1</sup> than that of SO<sub>3</sub>···H<sub>2</sub>O, thus leading to that the equilibrium constant of  
9 the former complex is larger by 1-2 orders of magnitude than that of the latter one in Table S2.  
10 Additionally, the larger equilibrium constant of H<sub>2</sub>SO<sub>4</sub>···H<sub>2</sub>O complex leads to its higher  
11 concentration in the atmosphere. For example, when the concentrations of SO<sub>3</sub> (Yao et al., 2020),  
12 H<sub>2</sub>SO<sub>4</sub> (Liu et al., 2015) and H<sub>2</sub>O (Anglada et al., 2013) were 10<sup>6</sup>, 10<sup>8</sup> and 10<sup>17</sup> molecules·cm<sup>-3</sup>,  
13 respectively, the concentrations of SO<sub>3</sub>···H<sub>2</sub>O and H<sub>2</sub>SO<sub>4</sub>···H<sub>2</sub>O were 2.41 × 10<sup>3</sup>-2.01 × 10<sup>4</sup> and  
14 5.01 × 10<sup>5</sup>-3.01 × 10<sup>8</sup> molecules·cm<sup>-3</sup> within the temperature range of 280-320 K (see Table S3),  
15 respectively. So, we predict that Channel DSA\_WM and Channel SA\_SA mainly take place via the  
16 collision of H<sub>2</sub>SO<sub>4</sub>···H<sub>2</sub>O with SO<sub>3</sub>. In order to check this prediction, the effective rate constants for  
17 two bimolecular reactions of H<sub>2</sub>SO<sub>4</sub>···H<sub>2</sub>O + SO<sub>3</sub> and SO<sub>3</sub>···H<sub>2</sub>O + H<sub>2</sub>SO<sub>4</sub> were calculated, and the  
18 details were shown in *SI Appendix*, Part 3 and Table 1. As seen in Table 1, the SO<sub>3</sub>···H<sub>2</sub>O + H<sub>2</sub>SO<sub>4</sub>  
19 reaction in both Channel DSA\_WM and Channel SA\_SA can be neglected as their effective rate  
20 constants are smaller by 16.7-48.5 and 1.02-3.05 times than the corresponding values in the  
21 H<sub>2</sub>SO<sub>4</sub>···H<sub>2</sub>O + SO<sub>3</sub> reaction within the temperature range of 280-320 K, respectively. Therefore,  
22 we only consider the H<sub>2</sub>SO<sub>4</sub>···H<sub>2</sub>O + SO<sub>3</sub> bimolecular reaction in both Channel DSA\_WM and  
23 Channel SA\_SA.”

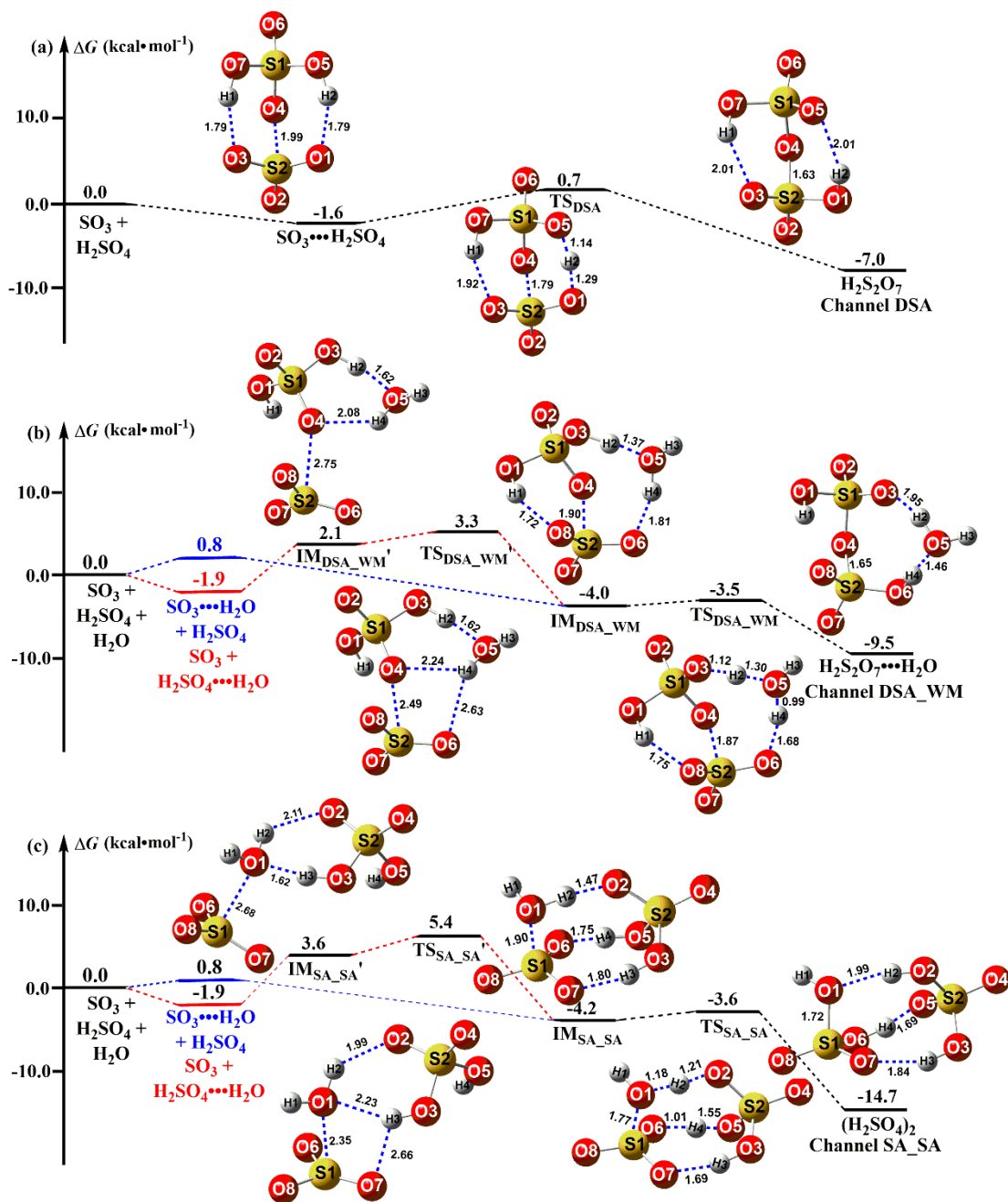
24 (c) As for the H<sub>2</sub>SO<sub>4</sub> formation from the SO<sub>3</sub> + H<sub>2</sub>SO<sub>4</sub> reaction with H<sub>2</sub>O, the discussion of  
25 the stepwise H<sub>2</sub>SO<sub>4</sub>···H<sub>2</sub>O + SO<sub>3</sub> reaction has been added in Lines 8-21 Page 10 of the revised  
26 manuscript, which has been reorganized as “Regarding Channel SA\_SA, the stepwise reaction  
27 occurred firstly via the ring enlargement from six-membered ring complex IM<sub>SA\_SA</sub>' to a cage-like  
28 hydrogen bonding network IM<sub>SA\_SA</sub>, and then took place by going through a transition state, TS<sub>SA\_SA</sub>,  
29 to from the product complex (H<sub>2</sub>SO<sub>4</sub>)<sub>2</sub>. TS<sub>DSA\_WM</sub> was in the middle of a double hydrogen transfer,  
30 where H<sub>2</sub>SO<sub>4</sub> acted as a bridge of hydrogen atom from the H<sub>2</sub>O to SO<sub>3</sub> along with O1 atom of H<sub>2</sub>O

1 addition to the S atom of SO<sub>3</sub>. It is worth noting that the energy barriers of two elementary reactions  
 2 involved in the stepwise route of Channel SA\_SA were only 1.8 and 0.6 kcal·mol<sup>-1</sup>, respectively,  
 3 showing that the stepwise route of Channel SA\_SA is feasible to take place from energetic point of  
 4 view.

5 (d) The discussion of the competition between the SO<sub>3</sub> + H<sub>2</sub>SO<sub>4</sub> reaction with H<sub>2</sub>O and the  
 6 hydrolysis of SO<sub>3</sub> with H<sub>2</sub>SO<sub>4</sub> have been discussed in Lines 8-14 Page 9 of the revised manuscript,  
 7 which has been reorganized as “To check whether Channel DSA\_WM is more favorable than  
 8 Channel SA\_SA or not, their rate ratio listed in Eq. 4 has been calculated in Table 1. The calculated  
 9 rate ratio  $\frac{v_{\text{DSA\_WM}_s}}{v_{\text{SA\_SA}_s}}$  shows that Channel DSA\_WM is more important than Channel SA\_SA  
 10 because the rate ratio  $\frac{v_{\text{DSA\_WM}_s}}{v_{\text{SA\_SA}_s}}$  is 1.53-3.04 within the temperature range of 280-320 K. So,  
 11 we predicted that the SO<sub>3</sub> + H<sub>2</sub>SO<sub>4</sub> reaction with H<sub>2</sub>O producing H<sub>2</sub>S<sub>2</sub>O<sub>7</sub> is more favorable than that  
 12 forming H<sub>2</sub>SO<sub>4</sub>.

$$13 \quad \frac{v_{\text{DSA\_WM}}}{v_{\text{SA\_SA}}} = \frac{v_{\text{DSA\_WM}_s} + v_{\text{DSA\_WM}_o}}{v_{\text{SA\_SA}_s} + v_{\text{SA\_SA}_o}} = \frac{k_{\text{DSA\_WM}_s} \times K_{\text{eq}(\text{H}_2\text{SO}_4 \cdots \text{H}_2\text{O})} + k_{\text{DSA\_WM}_o} \times K_{\text{eq}(\text{SO}_3 \cdots \text{H}_2\text{O})}}{k_{\text{SA\_SA}_s} \times K_{\text{eq}(\text{H}_2\text{SO}_4 \cdots \text{H}_2\text{O})} + k_{\text{SA\_SA}_o} \times K_{\text{eq}(\text{SO}_3 \cdots \text{H}_2\text{O})}} \quad (4)''$$

14 Overall, in the SO<sub>3</sub> + H<sub>2</sub>SO<sub>4</sub> reaction with H<sub>2</sub>O, a single water molecule both acting as a  
 15 catalyst and a reactant has been investigated. Meanwhile, these two kinds of reactions mainly take  
 16 place via the collision of H<sub>2</sub>SO<sub>4</sub>···H<sub>2</sub>O with SO<sub>3</sub>. Moreover, the SO<sub>3</sub> + H<sub>2</sub>SO<sub>4</sub> reaction with H<sub>2</sub>O  
 17 producing H<sub>2</sub>S<sub>2</sub>O<sub>7</sub> is more favorable than that forming H<sub>2</sub>SO<sub>4</sub> as the rate ratio  $\frac{v_{\text{DSA\_WM}}}{v_{\text{SA\_SA}}}$  is  
 18 1.53-3.04 within the temperature range of 280-320 K.



1

2

**Fig. 1** Schematic potential energy surface of the  $\text{SO}_3 + \text{H}_2\text{SO}_4$  reaction without and with  $\text{H}_2\text{O}$  at the CCSD(T)-F12/cc-pVDZ-F12//M06-2X/6-311+G(2df,2pd) level

3

**Table 1** The rate constant ( $\text{cm}^3 \cdot \text{molecule}^{-1} \cdot \text{s}^{-1}$ ) for the  $\text{SO}_3 + \text{H}_2\text{SO}_4$  reaction along with the effective rate constant ( $\text{cm}^3 \cdot \text{molecule}^{-1} \cdot \text{s}^{-1}$ ) for the  $\text{SO}_3 + \text{H}_2\text{SO}_4$  reaction with  $\text{H}_2\text{O}$  (100%RH) within the temperature range of 280-320 K

4

5

6

| $T(\text{K})$           | 280 K                  | 290 K                  | 298 K                  | 300 K                  | 310 K                  | 320 K                  |
|-------------------------|------------------------|------------------------|------------------------|------------------------|------------------------|------------------------|
| $k_{\text{DSA}}$        | $5.52 \times 10^{-12}$ | $4.60 \times 10^{-12}$ | $3.95 \times 10^{-12}$ | $3.80 \times 10^{-12}$ | $3.13 \times 10^{-12}$ | $2.57 \times 10^{-12}$ |
| $k'_{\text{DSA\_WM}_o}$ | $2.12 \times 10^{-13}$ | $2.68 \times 10^{-13}$ | $2.88 \times 10^{-13}$ | $2.89 \times 10^{-13}$ | $2.89 \times 10^{-13}$ | $2.75 \times 10^{-13}$ |
| $k'_{\text{DSA\_WM}_s}$ | $1.03 \times 10^{-11}$ | $8.55 \times 10^{-12}$ | $7.42 \times 10^{-12}$ | $7.11 \times 10^{-12}$ | $5.79 \times 10^{-12}$ | $4.60 \times 10^{-12}$ |
| $k'_{\text{SA\_SA}_o}$  | $1.29 \times 10^{-21}$ | $8.69 \times 10^{-22}$ | $6.00 \times 10^{-22}$ | $5.37 \times 10^{-22}$ | $3.47 \times 10^{-22}$ | $2.28 \times 10^{-22}$ |

|                                      |                        |                        |                        |                        |                        |                        |
|--------------------------------------|------------------------|------------------------|------------------------|------------------------|------------------------|------------------------|
| $k'_{SA\_SA\_s}$                     | $3.93 \times 10^{-21}$ | $1.82 \times 10^{-21}$ | $1.01 \times 10^{-21}$ | $8.62 \times 10^{-12}$ | $4.42 \times 10^{-12}$ | $2.34 \times 10^{-12}$ |
| $\frac{\nu_{DSA\_WM}}{\nu_{SA\_SA}}$ | 3.04                   | 2.61                   | 2.30                   | 2.22                   | 1.85                   | 1.53                   |

1  $k_{DSA}$  is the rate constant for the  $SO_3 + H_2SO_4$  reaction;  $k'_{DSA\_WM\_o}$  and  $k'_{DSA\_WM\_s}$  are respectively the effective rate  
2 constants for  $H_2O$ -assisted  $SO_3 + H_2SO_4$  reaction occurring through one-step and stepwise routes.  $k'_{SA\_SA\_o}$  and  
3  $k'_{SA\_SA\_s}$  are respectively the effective rate constants for the hydrolysis reaction of  $SO_3$  with  $H_2SO_4$  occurring through  
4 one-step and stepwise routes.  $\nu_{DSA\_WM}/\nu_{SA\_SA}$  is the rate ratio between Channel DSA\_WM and Channel SA\_SA.

5

6 **Comment 2.**

7 While interesting, I'm not sure the BOMD simulations are saying much about the relevance of  
8  $H_2S_2O_7$  for actual new-particle formation:  $H_2S_2O_7$  formed in water droplets will presumably stay  
9 there, and never evaporate to participate in NPF. (Overall, "air-water interfaces" have little to do  
10 with actual NPF, as the interfaces are by definition found in particles that \*have already formed\*:  
11 many of the claims of "NPF-relevance" made in the study are thus by definition incorrect). While  
12 there may be some relevance of the studied process to particle growth, even  $H_2SO_4$  has an essentially  
13 zero evaporation rate from any particles larger than a few nanometers - so it may make little  
14 difference to the growth of larger aerosol whether the sulfur is taken up as  $H_2SO_4$  or  $H_2S_2O_7$  (also  
15 see issue 4 for a further caveat).

16 **Response:** Thanks for your valuable comments. We agree with the suggestion of the reviewer that  
17 the reaction of  $H_2S_2O_7$  or  $H_2SO_4$  formations at air-water interface is not directly related to new  
18 particle formation. However, the reaction of  $H_2S_2O_7$  or  $H_2SO_4$  formations at air-water interface is  
19 necessary to investigate by using BOMD simulations. This is because that

20 (a) Many investigations (*J. Am. Chem. Soc.*, 2016, 138, 1816-1819; *Proc. Natl. Acad. Sci.*  
21 *U.S.A*, 2017, 114, 12401-12406.; *J. Am. Chem. Soc.*, 2018, 140, 6456-6466.; *J. Am. Chem. Soc.*,  
22 2018, 140, 14, 4913-4921.; *Chem. Sci.*, 2019, 10, 743-751.; *Chem. Sci.*, 2017,8, 5385-5391.)  
23 suggest that interfacial environment not only triggers the arrangement and aggregation of  
24 hydrophilic groups, but also provides a good medium for many atmospheric reactions. Notably, due  
25 to the induction of proton transfer pathways by interfacial water molecules, many atmospheric  
26 reactions that occur on the surface of aerosols and droplets are faster, and sometimes are different  
27 from the corresponding processes in the gas phase. Based on this, the differences in the reactivity  
28 of  $SO_3$  with  $H_2SO_4$  in the gas phase and at the air-water interface were evaluated by using BOMD  
29 simulations.

1 (b) The BOMD simulation results at the air-water interface suggest that three different types  
2 of interfacial reaction mechanisms (i) H<sub>2</sub>O-induced the formation of S<sub>2</sub>O<sub>7</sub><sup>2-</sup>···H<sub>3</sub>O<sup>+</sup> ion pair; (ii)  
3 HSO<sub>4</sub><sup>-</sup> mediated the formation of HSO<sub>4</sub><sup>-</sup>···H<sub>3</sub>O<sup>+</sup> ion pair and (iii) the deprotonation of H<sub>2</sub>S<sub>2</sub>O<sub>7</sub> were  
4 observed. These interfacial reactions occurred through stepwise mechanism to form the ion pair of  
5 S<sub>2</sub>O<sub>7</sub><sup>2-</sup>···H<sub>3</sub>O<sup>+</sup> and HSO<sub>4</sub><sup>-</sup>···H<sub>3</sub>O<sup>+</sup>, and proceed on the picosecond time scale. These interfacial  
6 mechanisms are in contrast to the gas phase reaction mechanisms in which loop-structure  
7 mechanism were involved in SO<sub>3</sub> + H<sub>2</sub>SO<sub>4</sub> reaction without and with H<sub>2</sub>O. Thus, the SO<sub>3</sub> + H<sub>2</sub>SO<sub>4</sub>  
8 reaction behavior at the air-water interface is different from that of the gas phase, and some new and  
9 different mechanisms have been found.

10 (c) Although the formation routes of the S<sub>2</sub>O<sub>7</sub><sup>2-</sup>···H<sub>3</sub>O<sup>+</sup> and HSO<sub>4</sub><sup>-</sup>···H<sub>3</sub>O<sup>+</sup> ion pair at air-water  
11 interface is not directly related to new particle formation, the S<sub>2</sub>O<sub>7</sub><sup>2-</sup> ion at the air-water interface  
12 has stronger nucleation potential as the following reasons. One reason is that the interactions of  
13 S<sub>2</sub>O<sub>7</sub><sup>2-</sup>···H<sub>2</sub>SO<sub>4</sub>, S<sub>2</sub>O<sub>7</sub><sup>2-</sup>···HNO<sub>3</sub>, S<sub>2</sub>O<sub>7</sub><sup>2-</sup>···(COOH)<sub>2</sub>, H<sub>3</sub>O<sup>+</sup>···NH<sub>3</sub>, H<sub>3</sub>O<sup>+</sup>···H<sub>2</sub>SO<sub>4</sub>, SA<sup>-</sup>···H<sub>2</sub>SO<sub>4</sub>, SA<sup>-</sup>  
14 ···(COOH)<sub>2</sub>, and SA<sup>-</sup>···HNO<sub>3</sub> listed in Table 2 are stronger than those of H<sub>2</sub>SO<sub>4</sub>···NH<sub>3</sub> (major  
15 precursor of atmospheric aerosols). These results reveal that interfacial S<sub>2</sub>O<sub>7</sub><sup>2-</sup>, SA<sup>-</sup> and H<sub>3</sub>O<sup>+</sup> can  
16 attract candidate species from the gas phase to the water surface. The other reason is that as  
17 compared with (SA)<sub>1</sub>(A)<sub>1</sub>(X)<sub>1</sub> (X = HOOCCH<sub>2</sub>COOH, HOCCOOSO<sub>3</sub>H, CH<sub>3</sub>OSO<sub>3</sub>H,  
18 HOOCCH<sub>2</sub>CH(NH<sub>2</sub>)COOH and HOCH<sub>2</sub>COOH) clusters (Zhong et al., 2019; Zhang et al., 2018;  
19 Rong et al., 2020; Gao et al., 2023; Liu et al., 2021a; Zhang et al., 2017), the number of hydrogen  
20 bonds in (SA)<sub>1</sub>(A)<sub>1</sub>(S<sub>2</sub>O<sub>7</sub><sup>2-</sup>)<sub>1</sub> cluster presented in Fig. S8 increased and the ring of the complex was  
21 enlarged. Meanwhile, comparing to (SA)<sub>1</sub>(A)<sub>1</sub>(X)<sub>1</sub> (X = HOOCCH<sub>2</sub>COOH, HOCCOOSO<sub>3</sub>H,  
22 CH<sub>3</sub>OSO<sub>3</sub>H, HOOCCH<sub>2</sub>CH(NH<sub>2</sub>)COOH and HOCH<sub>2</sub>COOH) clusters (Table 2), the Gibbs  
23 formation free energy ΔG of (SA)<sub>1</sub>(A)<sub>1</sub>(S<sub>2</sub>O<sub>7</sub><sup>2-</sup>)<sub>1</sub> cluster is lower, showing S<sub>2</sub>O<sub>7</sub><sup>2-</sup> ion at the air-water  
24 interface has stronger nucleation ability than X in the gas phase. Based on this, the sentence of “**and**  
25 **thus in turn accelerates the growth of particle.**” has been deleted in Line 14 Page 14 of the revised  
26 manuscript. Similarly, the sentence of “**enhancing potential of S<sub>2</sub>O<sub>7</sub><sup>2-</sup> on SA-A cluster**” has been  
27 changed as “**the nucleation potential of S<sub>2</sub>O<sub>7</sub><sup>2-</sup> on SA-A cluster**” in Line 15 Page 16 of the revised  
28 manuscript. Moreover, the sentence of “**the Gibbs formation free energy ΔG of (SA)<sub>1</sub>(A)<sub>1</sub>(S<sub>2</sub>O<sub>7</sub><sup>2-</sup>)<sub>1</sub>**  
29 **cluster is lower. Therefore, we predict that S<sub>2</sub>O<sub>7</sub><sup>2-</sup> at the air-water interface has important implication**  
30 **to the aerosol NPF in highly industrial polluted regions with high concentrations of SO<sub>3</sub>.**” has been

1 changed as “the Gibbs formation free energy  $\Delta G$  of  $(SA)_1(A)_1(S_2O_7^{2-})_1$  cluster is lower, showing  
2  $S_2O_7^{2-}$  ion at the air-water interface has stronger nucleation ability than  $X$  in the gas phase. Therefore,  
3 we predict that  $S_2O_7^{2-}$  at the air-water interface has stronger nucleation potential.” in Lines 23-26  
4 Page 16 of the revised manuscript.

5 Overall, the BOMD simulations of three different types of interfacial reaction mechanisms (*i*)  
6  $H_2O$ -induced the formation of  $S_2O_7^{2-}\cdots H_3O^+$  ion pair; (*ii*)  $HSO_4^-$  mediated the formation of  $HSO_4^-$   
7  $\cdots H_3O^+$  ion pair and (*iii*) the deprotonation of  $H_2S_2O_7$  were studied. These interfacial reactions  
8 occurred through stepwise mechanism and were in contrast to the gas phase reaction mechanisms  
9 in which loop-structure mechanism were involved in  $SO_3 + H_2SO_4$  reaction without and with  $H_2O$ .  
10 Then, the nucleation potential of  $S_2O_7^{2-}$  at the air-water interface has been investigated by  
11 considering the adsorption capacity of the  $S_2O_7^{2-}$ ,  $H_3O^+$  and  $SA^-$  to gaseous precursors in the  
12 atmosphere as well as the geometrical structure and the formation free energies of the  
13  $(SA)_1(A)_1(S_2O_7^{2-})_1$  clusters.

### 14 15 **Comment 3.**

16 The authors spend much time discussing the results they obtain for the “enhancement factor”  $R$   
17 (equation 5). As cautioned in Elm et al. (<https://www.sciencedirect.com/science/article/abs/pii/S0021850220301099>), the excessive use of such abstract “enhancement factors” is  
18 questionable and risky. In this particular case, I don’t believe the results are actually technically  
19 badly wrong - for example including the effect of  $H_2SO_4$  depletion (caused by a fraction of the  $SO_3$   
20 forming DSA rather than  $H_2SO_4$ ) would probably not change the qualitative results, as the clustering  
21 ability of DSA is much greater than that of  $H_2SO_4$ . (For completeness sake, I would nevertheless  
22 recommend this is done). However, many of the presented “results” are in reality rather trivial  
23 consequence of how the simulation is set up, and the parameters defined. For example, the  $R$  values  
24 are quite obviously “greater than or equal to 1”, as the  $J$  values with added DSA cannot (in the way  
25 the authors run ACDC) be lower than the  $J$  values without the added DSA. Similarly, the various  
26 correlations between  $R$  and different parameters are not particularly informative or novel. I  
27 recommend the authors first of all account for all relevant effects (including sulfur depletion - ie run  
28 the code with a constant  $SO_3$  source rather than constant  $[H_2SO_4]$ ), and also condense the discussion  
29 on “enhancement factors”.  
30



1 **Response:** Thanks for your valuable comments. The reason for using a constant SO<sub>3</sub> source is not  
2 reasonable has been explained firstly. Meanwhile, the corresponding discussion on “enhancement  
3 factors” have been condensed and the analysis of the absolute formation rate with temperature and  
4 concentration changes after the addition of H<sub>2</sub>S<sub>2</sub>O<sub>7</sub> has been added. The corresponding major  
5 revision has been made as follows.

6 (a) It is not reasonable to use a constant SO<sub>3</sub> source since there are many pathways for the  
7 removal of SO<sub>3</sub> removal processes. the hydrolysis of SO<sub>3</sub> to product H<sub>2</sub>SO<sub>4</sub> is the most major loss  
8 route of SO<sub>3</sub> in the atmosphere. As a complement to the loss of SO<sub>3</sub>, ammonolysis reaction of SO<sub>3</sub>  
9 in polluted areas of NH<sub>3</sub> can form H<sub>2</sub>NSO<sub>3</sub>H, which can be competitive with the formation of H<sub>2</sub>SO<sub>4</sub>  
10 from the hydrolysis reaction of SO<sub>3</sub>. Besides, the reactions of SO<sub>3</sub> with CH<sub>3</sub>OH, HNO<sub>3</sub>, and organic  
11 acids (e.g., formic acid, acetic acid and acrylic acid). These reactions consume some SO<sub>3</sub> in the  
12 atmosphere and inhibit the hydrolysis of SO<sub>3</sub> (H<sub>2</sub>SO<sub>4</sub> formation) to some extent. Thus, it is not  
13 suitable to use a constant source of SO<sub>3</sub>.

14 The concentration of H<sub>2</sub>S<sub>2</sub>O<sub>7</sub> has been re-evaluated within the altitude range of 0-30 km. Then,  
15 the analysis of the absolute formation rate with temperature and concentration changes after the  
16 addition of H<sub>2</sub>S<sub>2</sub>O<sub>7</sub> has been added in Lines 28-30 Page 14 to Lines 1-13 Page 15 of the revised  
17 manuscript, which has been organized as “The potential enhancement influence of DSA to the SA-  
18 A-based particle formation was shown in Fig. 6. The formation rate ( $J$ , cm<sup>-3</sup>·s<sup>-1</sup>) of SA-A-DSA-  
19 based system illustrated in Fig. 6 was negatively dependent on temperature, demonstrating that the  
20 low temperature is a key factor to accelerate cluster formation. It is noted that, at low temperatures  
21 of 218.15 K (Fig. S12) and 238.15 K (Fig. S13), the actual  $\Delta G$  of clusters has been calculated to  
22 ensure meaningful cluster dynamics of the 3 × 3 systems, where the actual  $\Delta G$  surface represented  
23 that the simulated set of clusters always included the critical cluster. In addition to temperature, the  
24  $J$  of SA-A-DSA-based system shown in Fig. 6 rise with the increase of [DSA]. More notably, the  
25 participation of DSA can promote  $J$  to a higher level, indicating its enhancement on SA-A  
26 nucleation. Besides, there was significantly positive dependence of the  $J$  of SA-A-DSA-based  
27 system on both [SA] and [A] in Fig. 7 (238.15 K) and Fig. S15-Fig. S18 (218.15, 258.15, 278.15  
28 and 298.15 K). This was because the higher concentration of nucleation precursors could lead to  
29 higher  $J$ . Besides, Fig. S19 showed the nucleation rate when the sum ([SA] + [DSA]) was kept  
30 constant.  $J_{\text{DSA/SA}}$  at substituted condition was higher than that at unsubstituted condition. These

1 results indicated that DSA may can greatly enhance the SA-A particle nucleation in heavy sulfur  
2 oxide polluted atmospheric boundary layer, especially at an average flight altitude of 10 km with  
3 high [DSA].”

4

#### 5 **Comment 4**

6 The most problematic part of the overall claim for atmospheric relevance is the neglect of H<sub>2</sub>S<sub>2</sub>O<sub>7</sub>  
7 decomposition by hydration (i.e. the H<sub>2</sub>S<sub>2</sub>O<sub>7</sub> + H<sub>2</sub>O ⇒ H<sub>2</sub>SO<sub>4</sub> + H<sub>2</sub>SO<sub>4</sub> reaction), which is very  
8 well known (e.g. from industrial sulfur chemistry) to be rapid and spontaneous. (Indeed, H<sub>2</sub>S<sub>2</sub>O<sub>7</sub> is  
9 one of the strongest dehydrating agents in the known universe - its hydration reaction is so strong  
10 and favourable that it can even extract water molecules from sugar.) The BOMD simulations  
11 indicate that H<sub>2</sub>S<sub>2</sub>O<sub>7</sub> is stable for 10 picoseconds - but this is nowhere near enough time for a H<sub>2</sub>S<sub>2</sub>O<sub>7</sub>  
12 to, for example, collide with a H<sub>2</sub>SO<sub>4</sub> (timescale: seconds) in the gas phase (and thus participate in  
13 NPF). Recently, another group showed that preliminary results on the role of sulfamic acid in new-  
14 particle formation are invalidated by rapid hydrolysis ([https://pubs.acs.org/doi/full/10.1021/acs.jpca.](https://pubs.acs.org/doi/full/10.1021/acs.jpca.3c04982)  
15 [3c04982](https://pubs.acs.org/doi/full/10.1021/acs.jpca.3c04982)) - I anticipate something very similar may end up being the case for di/pyrosulfuric acid  
16 in the Earth’s lower atmosphere. Having said that, the presented results may very well have  
17 relevance for stratospheric chemistry, as well as for cloud chemistry on Venus (where there is much  
18 less water, and much more H<sub>2</sub>SO<sub>4</sub>). I recommend the atmospheric implications and relevance  
19 discussion be reformulated to target the appropriate atmospheres /or regions of them. Or at the very  
20 least, the possible (even likely) rapid hydrolysis of H<sub>2</sub>S<sub>2</sub>O<sub>7</sub> should be mentioned as a major caveat  
21 of the results (and as a strongly recommended subject for follow-up studies!)

22 **Response:** Thanks for your valuable comments. According to the reviewer’s suggestion, the  
23 importance of the SO<sub>3</sub> + H<sub>2</sub>SO<sub>4</sub> reaction has been investigated in the atmospheres of Earth and Venus.  
24 Meanwhile, the concentration of H<sub>2</sub>S<sub>2</sub>O<sub>7</sub> has been re-evaluated where the end and outside the  
25 aircraft engine and flight was considered. The corresponding revision has been made as follows.

26 (a) To understand the competition between the SO<sub>3</sub> + H<sub>2</sub>SO<sub>4</sub> reaction and H<sub>2</sub>O-assisted  
27 hydrolysis of SO<sub>3</sub> in the Earth’s atmosphere, the rate ratio (v<sub>DSA</sub>/v<sub>SA</sub>) between the SO<sub>3</sub> + H<sub>2</sub>SO<sub>4</sub>  
28 reaction and H<sub>2</sub>O-assisted hydrolysis of SO<sub>3</sub> has been calculated and was expressed in Eq. (5).

29 
$$\frac{v_{\text{DSA}}}{v_{\text{SA}}} = \frac{k_{\text{DSA}} \times [\text{SO}_3] \times [\text{H}_2\text{SO}_4] + k_{\text{DSA\_WM\_s}} \times K_{\text{eq1}} \times [\text{SO}_3] \times [\text{H}_2\text{SO}_4] \times [\text{H}_2\text{O}]}{k_{\text{SA\_WM}} \times K_{\text{eq2}} \times [\text{SO}_3] \times [\text{H}_2\text{O}] \times [\text{H}_2\text{O}]} \quad (5)$$

1 In Eq. (5),  $K_{eq1}$  and  $K_{eq2}$  were the equilibrium constant for the formation of  $H_2SO_4 \cdots H_2O$  and  
2  $SO_3 \cdots H_2O$  complexes shown in Table S2, respectively;  $k_{DSA}$ ,  $k_{DSA\_WM\_s}$  and  $k_{SA\_WM}$  were  
3 respectively denoted the bimolecular rate coefficient for the  $H_2SO_4 + SO_3$ ,  $H_2SO_4 \cdots H_2O + SO_3$  and  
4  $SO_3 \cdots H_2O + H_2O$  reactions;  $[H_2O]$  and  $[H_2SO_4]$  were respectively represented the concentration of  
5  $H_2O$  and  $H_2SO_4$  taken from references (*J. Phys. Chem. A*, 2013, 117, 10381-10396.; *Environ. Sci.*  
6 *Technol.*, 2015, 49, 13112-13120.). The corresponding rate ratio have been listed in Table S7 (0 km  
7 altitude) and S8 (5-30 km altitude). As seen in Table S7, at 0 km altitude, the hydrolysis reaction of  
8  $SO_3$  with  $(H_2O)_2$  is more favorable than the  $SO_3 + H_2SO_4$  reaction as the  $[H_2O]$  ( $10^{16}$ - $10^{18}$   
9  $molecules \cdot cm^3$ ) is much larger than that of  $[H_2SO_4]$  ( $10^4$ - $10^8$   $molecules \cdot cm^3$ ). Although the  
10 concentration of water molecules decreases with the increase of altitude in Table S8, the  
11 concentration of  $[H_2O]$  is still much greater than that of  $[H_2SO_4]$ , resulting in the  $SO_3 + H_2SO_4$   
12 reaction cannot compete with  $H_2O$ -assisted hydrolysis of  $SO_3$  within the altitude range of 5-30 km.  
13 Moreover, the  $SO_3 + H_2SO_4$  reaction is not also the major sink route of  $SO_3$ , even considering of  
14 high  $H_2SO_4$  concentration at the end and outside the aircraft engine and flight. Based on this, the  
15 sentence of “The value of  $v_{DSA}/v_{SA}$  was listed in Table S7 (0 km altitude) and S8 (5-30 km altitude).  
16 As seen in Table S7, at 0 km altitude, the hydrolysis reaction of  $SO_3$  with  $(H_2O)_2$  is more favorable  
17 than the  $SO_3 + H_2SO_4$  reaction as the  $[H_2O]$  ( $10^{16}$ - $10^{18}$   $molecules \cdot cm^3$ ) is much larger than that of  
18  $[H_2SO_4]$  ( $10^4$ - $10^8$   $molecules \cdot cm^3$ ). Although the concentration of water molecules decreases with  
19 the increase of altitude in Table S8, the concentration of  $[H_2O]$  is still much greater than that of  
20  $[H_2SO_4]$ , resulting in the  $SO_3 + H_2SO_4$  reaction cannot compete with  $H_2O$ -assisted hydrolysis of  
21  $SO_3$  within the altitude range of 5-30 km. Even considering of high  $H_2SO_4$  concentration at the end  
22 and outside the aircraft engine and flight at 10 km, the  $SO_3 + H_2SO_4$  reaction is not also the major  
23 sink route of  $SO_3$ .” has been added in Lines 24-29 Page 13 to Lines 1-4 Page 14 of the revised  
24 manuscript.

25 (b) It has been proposed that the concentration of sulfuric acid is even greater than that of water  
26 vapor in the atmosphere of Venus (*Science*, 1990, 249, 1273.; *Planet. Space Sci.*, 2006, 54, 1352.;  
27 *Icarus*, 1994, 109, 58.; *Nat. Geosci.*, 2010, 3, 834.), which may lead to that the  $SO_3 + H_2SO_4$  reaction  
28 is probably favorable than the  $H_2O$ -assisted hydrolysis of  $SO_3$  in the Venus’ atmosphere. To check  
29 whether the  $SO_3 + H_2SO_4$  reaction is more favorable than  $H_2O$ -assisted hydrolysis of  $SO_3$  or not in  
30 the Venus’ atmosphere, the rate ratio of  $v_{DSA}/v_{SA}$  listed in Eq. 4 has been calculated in Table 2. It

1 can be seen from Table 2 that the rate ratio of  $v_{\text{DSA}}/v_{\text{SA}}$  is  $3.24 \times 10^8$ - $5.23 \times 10^{10}$  in the 40-70 km  
2 altitude range of Venus, which indicates that the  $\text{SO}_3 + \text{H}_2\text{SO}_4$  reaction is significantly more  
3 favorable than the hydrolysis reaction of  $\text{SO}_3 + (\text{H}_2\text{O})_2$  within the altitudes range of 40-70 km in the  
4 Venus' atmosphere. Based on this, the sentence of “Notably, as the concentration of sulfuric acid is  
5 even greater than that of water vapor in the atmosphere of Venus, the  $\text{SO}_3 + \text{SA}$  reaction is probably  
6 favorable than the  $\text{H}_2\text{O}$ -assisted hydrolysis of  $\text{SO}_3$  in the Venus' atmosphere. To check whether the  
7  $\text{SO}_3 + \text{H}_2\text{SO}_4$  reaction is more favorable than  $\text{H}_2\text{O}$ -assisted hydrolysis of  $\text{SO}_3$  or not in the Venus'  
8 atmosphere, the rate ratio of  $v_{\text{DSA}}/v_{\text{SA}}$  listed in Eq. 4 has been calculated in Table 2. It can be seen  
9 from Table 2 that the rate ratio of  $v_{\text{DSA}}/v_{\text{SA}}$  is  $3.24 \times 10^8$ - $5.23 \times 10^{10}$  in the 40-70 km altitude range  
10 of Venus, which indicates that the  $\text{SO}_3 + \text{H}_2\text{SO}_4$  reaction is significantly more favorable than the  
11 hydrolysis reaction of  $\text{SO}_3 + (\text{H}_2\text{O})_2$  within the altitudes range of 40-70 km in the Venus' atmosphere.”  
12 has been added in Lines 4-11 Page 14 of the revised manuscript.

13 (c) Considering the concentration of sulfuric acid at the end and outside the aircraft engine and  
14 flight (up to 600 pptv), the concentration of  $\text{H}_2\text{S}_2\text{O}_7$  has been re-evaluated within the altitude range  
15 of 0-30 km. Specifically, the steady-state concentration of DSA was calculated using the calculated  
16 equilibrium constant listed in Eq. S5.

$$17 \quad K_{\text{eq}3} = \frac{[\text{DSA}]}{[\text{SO}_3][\text{SA}]} \quad (\text{S5})$$

18 where  $K_{\text{eq}3}$  is the equilibrium constant of DSA with respect to  $\text{SO}_3$  and  $\text{H}_2\text{SO}_4$  within the altitude  
19 range of 0-30 km shown in Table S9;  $[\text{SO}_3]$ ,  $[\text{SA}]$  and  $[\text{DSA}]$  are the concentrations of  $\text{SO}_3$ ,  $\text{H}_2\text{SO}_4$ ,  
20 and  $\text{H}_2\text{S}_2\text{O}_7$ , respectively. Although the concentration of sulfur trioxide remains unknown at  
21 different altitudes, experimental observations have shown that the concentration of sulfur trioxide  
22 can reach  $10^6$  molecules  $\text{cm}^{-3}$  in the troposphere. Moreover, water vapor concentrations significantly  
23 decrease with increasing of altitude. Consequently, the concentration of sulfur trioxide should be  
24 higher in the stratosphere than in the troposphere, and its concentration would increase as a result  
25 of geoengineered injection of  $\text{SO}_2$  or  $\text{SO}_3$ . Besides, it is worth noting that  $\text{H}_2\text{SO}_4$  can form at the  
26 end and outside the engine, and flight measurements in the exhaust plume have measured sulfuric  
27 acid abundances up to a value of 600 pptv. When an average flight altitude of 10 km is considered,  
28 this corresponds to a concentration of  $5.1 \times 10^9$  molecules  $\cdot \text{cm}^{-3}$ . Therefore, we have calculated the  
29 concentrations of DSA according to concentrations of sulfur trioxide in the range from  $10^7$  to  $10^{14}$

1 molecules  $\text{cm}^{-3}$  and the concentrations of  $\text{H}_2\text{SO}_4$  in the range of  $10^4$ - $10^9$  molecules  $\text{cm}^{-3}$  as shown  
2 in Fig. S9.

3 The maximum concentration of DSA displayed in Fig. S9 can be up to  $10^8$  molecules  $\cdot \text{cm}^{-3}$ .  
4 However, it should be noted that the concentration of water in the troposphere is abundant, and DSA  
5 is easily hydrolyzed to form  $\text{H}_2\text{SO}_4$ . Based on this, the concentration of DSA listed in Fig. S9 was  
6 overestimated. However, the extent and proportion of DSA hydrolysis remains unclear, and the  
7 hydrolysis behavior of DSA needs to be further investigated in subsequent studies. Therefore, the  
8 maximum concentration of DSA ( $10^8$  molecules  $\cdot \text{cm}^{-3}$ ) was not included in the effect of  $\text{H}_2\text{S}_2\text{O}_7$ , the  
9 product of the reaction between  $\text{SO}_3$  and  $\text{H}_2\text{SO}_4$ , on new particle formation (NPF) in various  
10 environments by using the Atmospheric Cluster Dynamics Code kinetic model and the QC  
11 calculation. In Lines 27-29 Page 7 to Lines 1-2 Page 8 of the revised manuscript, the discussion of  
12 the DSA concentration has been added as “As the prediction in Table S7, the concentration of DSA  
13 is set to  $10^4$ - $10^8$  molecules  $\cdot \text{cm}^{-3}$ . However, DSA is easily hydrolyzed with abundant water in the  
14 troposphere to form  $\text{H}_2\text{SO}_4$ , the concentration of DSA listed in Fig. S9 was overestimated. So, the  
15 maximum concentration of DSA ( $10^8$  molecules  $\cdot \text{cm}^{-3}$ ) was not included in the effect of  $\text{H}_2\text{S}_2\text{O}_7$  on  
16 new particle formation (NPF) in various environments.”

17 Overall, the  $\text{SO}_3 + \text{SA}$  reaction cannot compete with  $\text{H}_2\text{O}$ -assisted hydrolysis of  $\text{SO}_3$  within the  
18 altitude range of 0-30 km in the Earth's atmosphere, even considering of high  $\text{H}_2\text{SO}_4$  concentration  
19 at the end and outside the aircraft engine and flight. However, the  $\text{SO}_3 + \text{SA}$  reaction is significantly  
20 more favorable than the hydrolysis reaction of  $\text{SO}_3 + (\text{H}_2\text{O})_2$  within the altitude range of 40-70 km  
21 in Venus' atmosphere. Moreover, as the extent and proportion of DSA hydrolysis is unclear, the  
22 maximum concentration of DSA ( $10^8$  molecules  $\cdot \text{cm}^{-3}$ ) was not included in the effect of  $\text{H}_2\text{S}_2\text{O}_7$  on  
23 new particle formation (NPF) in various environments by using the Atmospheric Cluster Dynamics  
24 Code kinetic model and the QC calculation.

25

#### 26 **Comment 5.**

27 Another issue to consider is the timescale associated with participation in NPF of compounds with  
28 mixing ratios well below a part per quadrillion. The gas-kinetic bimolecular collision rate for small  
29 molecules and their clusters is around  $1\text{E}-10$ ... $1\text{E}-9$   $\text{cm}^3$  per molecule and second. If the DSA  
30 concentration is 1 molecule per  $\text{cm}^3$ , then on average a  $\text{H}_2\text{SO}_4$  molecule, or a  $\text{H}_2\text{SO}_4$ -containing

1 cluster, will thus collide with DSA molecules about once per 1E9 seconds or so (as the pseudo-  
2 unimolecular collision rate is  $k_{\text{coll}}$  times the concentration, and the lifetime with respect to  
3 collisions is the inverse of this). This is more than 30 YEARS. Even for a DSA concentration of 10  
4 per  $\text{cm}^3$ , the timescale of a given molecule or cluster colliding with a DSA molecule is more than 3  
5 YEARS. Or for 100 per  $\text{cm}^3$ , more than 3 months. It is quite clear from this that the pseudo-steady-  
6 state assumed by ACDC simulations will simply never have time to form, when some of the  
7 participating molecules have such low concentrations. Or in other words, the basic assumptions  
8 required for modelling clustering with ACDC do not apply in these cases (or, to put it yet another  
9 way, an ACDC - type code needs to be run in a very different way, explicitly accounting for these  
10 timescales).

11 **Response:** Thanks for your valuable comments. We agree with the reviewer that at some of the  
12 participating molecules such low concentrations that the pseudo-steady-state assumed by ACDC  
13 simulations will simply never have time to form. Based on this, Considering the concentration of  
14 sulfuric acid at the end and outside the aircraft engine and flight (up to 600 pptv), the concentration  
15 of  $\text{H}_2\text{S}_2\text{O}_7$  has been re-evaluated within the altitude range of 0-30 km. Specifically, the steady-state  
16 concentration of DSA was calculated using the calculated equilibrium constant listed in Eq. S5.

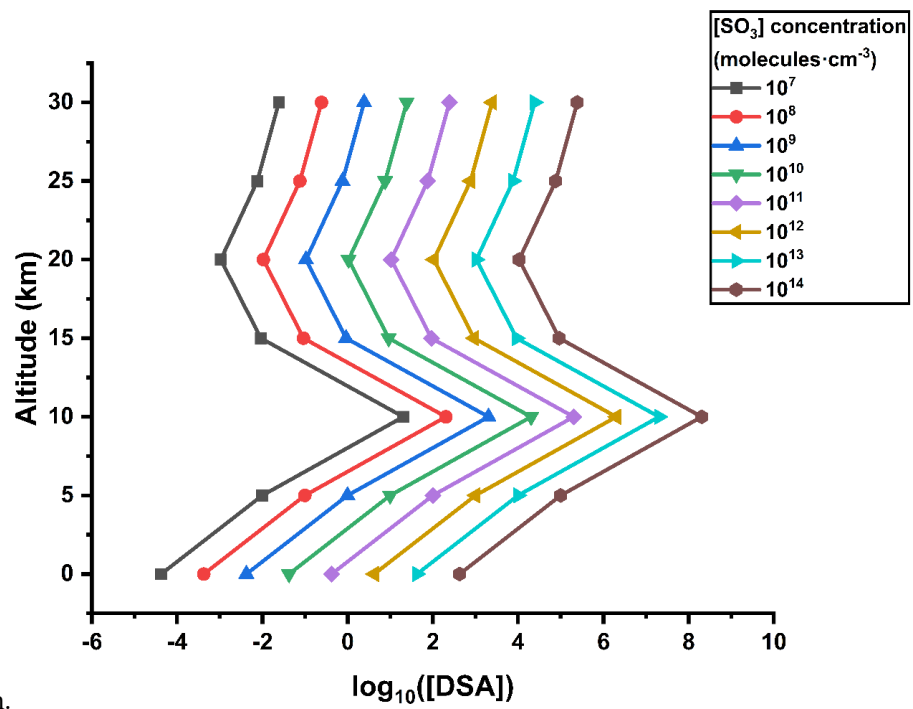
$$17 \quad K_{\text{eq}3} = \frac{[\text{DSA}]}{[\text{SO}_3][\text{SA}]} \quad (\text{S5})$$

18 where  $K_{\text{eq}3}$  is the equilibrium constant of DSA with respect to  $\text{SO}_3$  and  $\text{H}_2\text{SO}_4$  within the altitude  
19 range of 0-30 km shown in Table S9;  $[\text{SO}_3]$ ,  $[\text{SA}]$  and  $[\text{DSA}]$  are the concentrations of  $\text{SO}_3$ ,  $\text{H}_2\text{SO}_4$ ,  
20 and  $\text{H}_2\text{S}_2\text{O}_7$ , respectively. Although the concentration of sulfur trioxide remains unknown at  
21 different altitudes, experimental observations have shown that the concentration of sulfur trioxide  
22 can reach  $10^6$  molecules  $\text{cm}^{-3}$  in the troposphere. Moreover, water vapor concentrations significantly  
23 decrease with increasing of altitude. Consequently, the concentration of sulfur trioxide should be  
24 higher in the stratosphere than in the troposphere, and its concentration would increase as a result  
25 of geoengineered injection of  $\text{SO}_2$  or  $\text{SO}_3$ . Besides, it is worth noting that  $\text{H}_2\text{SO}_4$  can form at the  
26 end and outside the engine, and flight measurements in the exhaust plume have measured sulfuric  
27 acid abundances up to a value of 600 pptv. When an average flight altitude of 10 km is considered,  
28 this corresponds to a concentration of  $5.1 \times 10^9$  molecules  $\cdot \text{cm}^{-3}$ . Therefore, we have calculated the  
29 concentrations of DSA according to concentrations of sulfur trioxide in the range from  $10^7$  to  $10^{14}$

1 molecules  $\text{cm}^{-3}$  and the concentrations of  $\text{H}_2\text{SO}_4$  in the range of  $10^4$ - $10^9$  molecules  $\text{cm}^{-3}$  as shown  
2 in Fig. S9.

3 The maximum concentration of DSA displayed in Fig. S9 can be up to  $10^8$  molecules  $\cdot \text{cm}^{-3}$ .

4 However, it should be noted that the concentration of water in the troposphere is abundant, and  
5 DSA is easily hydrolyzed to form  $\text{H}_2\text{SO}_4$ . Based on this, the concentration of DSA listed in Fig. S9  
6 was overestimated. The extent and proportion of DSA hydrolysis remains unclear, and the  
7 hydrolysis behavior of DSA needs to be further investigated in subsequent studies. Therefore, the  
8 maximum concentration of DSA ( $10^8$  molecules  $\cdot \text{cm}^{-3}$ ) was not included in the effect of  $\text{H}_2\text{S}_2\text{O}_7$ ,  
9 the product of the reaction between  $\text{SO}_3$  and  $\text{H}_2\text{SO}_4$ , on new particle formation (NPF) in various  
10 environments by using the Atmospheric Cluster Dynamics Code kinetic model and the QC



11 calculation.

12 **Fig. S9** Concentration (unit: molecules  $\cdot \text{cm}^{-3}$ ) of DSA with respect to different concentrations of  $\text{SO}_3$   
13 as function of altitude. We consider the possible concentrations of  $\text{SO}_3$  with the injection of  $\text{SO}_3$ .

15 The maximum concentration of DSA displayed in Fig. S9 can be up to  $10^8$  molecules  $\cdot \text{cm}^{-3}$ .

16 However, it should be noted that the concentration of water in the troposphere is abundant, and DSA  
17 is easily hydrolyzed to form  $\text{H}_2\text{SO}_4$ . Based on this, the concentration of DSA listed in Fig. S9 was  
18 overestimated. The extent and proportion of DSA hydrolysis remains unclear, and the hydrolysis  
19 behavior of DSA needs to be further investigated in subsequent studies. Therefore, the maximum  
20 concentration of DSA ( $10^8$  molecules  $\cdot \text{cm}^{-3}$ ) was not included in the effect of  $\text{H}_2\text{S}_2\text{O}_7$ , the product of

1 the reaction between SO<sub>3</sub> and H<sub>2</sub>SO<sub>4</sub>, on new particle formation (NPF) in various environments by  
2 using the Atmospheric Cluster Dynamics Code kinetic model and the QC calculation.

#### 3 4 **Technical issues**

##### 5 **Comment 6.**

6 The kinetic approach used here seems quite elaborate, given that the authors are not actually treating  
7 (or at least not discussing) any sort of pressure dependence, non-thermalisation, etc. How different  
8 are the rates compared to what one would obtain using a simple transition state theory framework  
9 (plus assuming kinetic gas theory forward rates for the initial complex formation)? I'm not  
10 criticising the use of elaborate methods as such, I'm just trying to assess how much difference they  
11 make, compared to a much simpler approach.

12 **Response:** Thanks for your valuable comments. The Rice-Ramsperger-Kassel-Marcus based  
13 Master Equation (ME/RRKM) model is well suited to calculate the kinetics of the SO<sub>3</sub> + H<sub>2</sub>SO<sub>4</sub>  
14 reaction without and with H<sub>2</sub>O. Specifically, as for the SO<sub>3</sub> + H<sub>2</sub>SO<sub>4</sub> → H<sub>2</sub>S<sub>2</sub>O<sub>7</sub> reaction without  
15 and with H<sub>2</sub>O illustrated in Fig. 1, the reaction without H<sub>2</sub>O has only a barrier height of 2.3 kcal·mol<sup>-1</sup>  
16 to produce the formation of H<sub>2</sub>S<sub>2</sub>O<sub>7</sub>, while the reaction with H<sub>2</sub>O only has a lower barrier height  
17 of 0.5 kcal·mol<sup>-1</sup>. It is reported that the ME/RRKM model has been used widely to calculate the rate  
18 constants of many gas phase reactions (*J. Am. Chem. Soc.*, 2022, 144, 19910-19920.; *J. Am. Chem.*  
19 *Soc.*, 2022, 144, 20, 9172-9177.; *Phys. Chem. Chem. Phys.*, 2022, 24, 18205-18216.; *Phys. Chem.*  
20 *Chem. Phys.*, 2022, 24, 4966-4977.; *J. Phys. Chem. A*, 2019, 123, 3131-3141.; *Chem. Phys. Lett.*,  
21 2020, 742, 137157.) where the rate constants for barrierless or near barrierless bimolecular reactions  
22 were evaluated reliably. In this case, the pre-equilibrium approximation used in our calculation is  
23 truly obsolete and may not be appropriate.

24 Meanwhile, to check the reliability of Master Equation (ME/RRKM) model, the rate constants  
25 for the SO<sub>3</sub> + H<sub>2</sub>SO<sub>4</sub> reaction without and with H<sub>2</sub>O were also calculated by using transition state  
26 theory (TST) coupled with the pre-equilibrium approximation. As seen in Table S6, the rate  
27 constants for the SO<sub>3</sub> + H<sub>2</sub>SO<sub>4</sub> reaction without and with H<sub>2</sub>O by using transition state theory is  
28 significantly higher than the gas kinetic limit. In addition, as for the rate constants calculated by  
29 transition state theory (TST) coupled with the pre-equilibrium approximation, the rate constants for  
30 the SO<sub>3</sub> + H<sub>2</sub>SO<sub>4</sub> reaction without and with H<sub>2</sub>O showed appreciably high negative temperature



1 dependence making the rate constants even larger at lower temperatures. This reveals that the TST  
 2 coupled with pre-equilibrium approximation used in our calculation is truly obsolete and may not  
 3 be appropriate. Thus, Using the Master Equation/Rice-Ramsperger-Kassel-Marcus (ME/RRKM)  
 4 models, the kinetic calculations for the SO<sub>3</sub> + H<sub>2</sub>SO<sub>4</sub> reaction without and with H<sub>2</sub>O were performed  
 5 by Barts-Widom method in the MESMER program package (Master Equation Solver for Multi-  
 6 Energy Well Reactions).

7 **Table S6** The rate constant (cm<sup>3</sup>·molecule<sup>-1</sup>·s<sup>-1</sup>) for the SO<sub>3</sub> + H<sub>2</sub>SO<sub>4</sub> reaction for the SO<sub>3</sub> + H<sub>2</sub>SO<sub>4</sub>  
 8 reaction without and with H<sub>2</sub>O within the temperature range of 280-320 K by using transition state  
 9 theory

| <i>T</i> /(K)                 | 280 K                   | 290 K                   | 298 K                   | 300 K                   | 310 K                   | 320 K                    |
|-------------------------------|-------------------------|-------------------------|-------------------------|-------------------------|-------------------------|--------------------------|
| <i>k</i> <sub>DSA</sub>       | 8.98 × 10 <sup>-9</sup> | 4.38 × 10 <sup>-9</sup> | 2.56 × 10 <sup>-9</sup> | 2.25 × 10 <sup>-9</sup> | 1.20 × 10 <sup>-9</sup> | 6.72 × 10 <sup>-10</sup> |
| <i>k'</i> <sub>DSA_WM_o</sub> | 5.77 × 10 <sup>-8</sup> | 2.59 × 10 <sup>-8</sup> | 1.42 × 10 <sup>-8</sup> | 1.23 × 10 <sup>-8</sup> | 6.12 × 10 <sup>-9</sup> | 3.18 × 10 <sup>-9</sup>  |
| <i>k'</i> <sub>DSA_WM_s</sub> | 5.20 × 10 <sup>-5</sup> | 2.44 × 10 <sup>-5</sup> | 1.39 × 10 <sup>-5</sup> | 1.21 × 10 <sup>-5</sup> | 6.29 × 10 <sup>-6</sup> | 3.42 × 10 <sup>-6</sup>  |

10 *k*<sub>DSA</sub> is the rate constant for the SO<sub>3</sub> + H<sub>2</sub>SO<sub>4</sub> reaction; *k*<sub>DSA\_WM\_o</sub> and *k*<sub>DSA\_WM\_s</sub> are respectively the rate constants  
 11 for H<sub>2</sub>O-assisted SO<sub>3</sub> + H<sub>2</sub>SO<sub>4</sub> reaction occurring through one-step and stepwise routes.

12  
 13 **Comment 7**

14 The method references for M06-2X, CCSD(T)-F12, and the ORCA program are not correct - the  
 15 first is completely wrong, while the latter refer to studies which have also used these approaches.  
 16 Please refer to the actual publications introducing the methods/codes instead.

17 **Response:** Thanks for your valuable comments. We are very sorry for using wrong references for  
 18 M06-2X, CCSD(T)-F12, and the ORCA program. The references regarding for the M06-2X,  
 19 CCSD(T)-F12 and the ORCA program has been respectively made as follows.

20 (a) As for M06-2X method, the correct references have been recited which has been organized  
 21 as references (Zhao and Truhlar, 2008; Elm et al., 2012).

22 [1] Zhao, Y., and Truhlar, D. G.: The M06 suite of density functionals for main group  
 23 thermochemistry, thermochemical kinetics, noncovalent interactions, excited states, and transition  
 24 elements: two new functionals and systematic testing of four M06-class functionals and 12 other  
 25 functionals, *Theor. Chem. Acc.*, 120, 215-241, 2008.;

26 [2] Elm, J., Bilde, M., and Mikkelsen, K. V.: Assessment of density functional theory in  
 27 predicting structures and free energies of reaction of atmospheric prenucleation clusters, *J. Chem.*  
 28 *Theory Comput.*, 8, 2071-2077, 2012.

1 (b) Regarding for CCSD(T)-F12 method, the relevant references have been changed which has  
2 been organized as references (Adler et al., 2007; Knizia et al., 2009).

3 [1] Adler, T. B., Knizia, G., and Werner, H. J.: A simple and efficient CCSD(T)-F12  
4 approximation, *J. Chem. Phys.*, 127, 221106, 10.1063/1.2817618, 2007.

5 [2] Knizia, G., Adler, T. B., and Werner, H.-J.: Simplified CCSD(T)-F12 methods: Theory and  
6 benchmarks, *J. Chem. Phys.*, 130, 054104, 10.1063/1.3054300, 2009.

7 (c) As for ORCA program, the corresponding reference have been recited which has been  
8 organized as references (Neese, 2012).

9 [1] Neese, F.: The ORCA program system, *WIREs Comput. Mol. Sci.*, 2, 73-78,  
10 <https://doi.org/10.1002/wcms.81>, 2012.

1 **Responses to Referee #2's comments**

2 We are grateful to the reviewers for their valuable and helpful comments on our manuscript  
3 "Reaction of SO<sub>3</sub> with H<sub>2</sub>SO<sub>4</sub> and Its Implication for Aerosol Particle Formation in the Gas Phase  
4 and at the Air-Water Interface" (MS No.: **egusphere-2023-2009**). We have revised the manuscript  
5 carefully according to reviewers' comments. The point-to-point responses to the Referee #2's  
6 comments are summarized below:

7

8 **Referee Comments**

9 Using computational methods Wang and co-workers study the reaction between H<sub>2</sub>SO<sub>4</sub> and  
10 SO<sub>3</sub> leading to the formation of H<sub>2</sub>S<sub>2</sub>O<sub>7</sub>. The gas-phase formation mechanism is studied using  
11 well-established methodologies, both with and without a water molecule present. The reaction is  
12 also studied at the air-water interface using Born-Oppenheimer molecular dynamics simulations.  
13 Finally, the authors study the potential of the formed H<sub>2</sub>S<sub>2</sub>O<sub>7</sub> product in "enhancing" new particle  
14 formation involving sulfuric acid and ammonia.

15 Overall, the applied quantum chemical methods are up to the current standard and the study is  
16 broadly atmospherically interesting, but I believe many of the conclusions are erroneously drawn  
17 and not supported by the data. Remember negative results are equally as important as positive  
18 results. So try to frame the results in a more transparent fashion. In addition, there is heavy  
19 referencing to the SI, which makes the paper difficult to follow in some places and the reader is  
20 left wondering if the claims are actually correct. I believe the paper might be worth publishing, but  
21 some critical changes must made.

22 **Response:** We would like to thank the reviewer for the positive and valuable comments, and we  
23 have revised our manuscript accordingly.

24

25 **Specific Comments:**

26 **Comment 1.**

27 **Overall:** When referring to the SI, please add the numbers to the text as well and elaborate on  
28 what the reader is supposed to look at in the SI. In several places it is very difficult to comprehend  
29 how the authors draw the conclusions.

1 **Response:** Thanks for your valuable comments. According to the reviewer's suggestion, the  
2 numbers have been added to the manuscript in reference to the SI and detailing what the reader  
3 should look for in the SI. The corresponding revision has been respectively made as follows.

4 (a) In Lines 18-19 Page 5 of the revised manuscript, the optimized structures and the  
5 formation Gibbs free energy of the stable clusters in the supporting information has been  
6 mentioned and organized as “The optimized structures and the formation Gibbs free energy of the  
7 stable clusters were summarized in Fig. S9 and Table S8 of the *SI Appendix*, respectively.”

8 (b) In Lines 18-19 Page 5 of the revised manuscript, the details of the equilibrium process  
9 for the droplet system with 191 water molecules in the supporting information has been mentioned  
10 and organized as “The details of the equilibrium process for the droplet system with 191 water  
11 molecules are shown in the *SI Appendix Part 4*.”

12 (c) In Lines 10-12 Page 9 of the revised manuscript, the details for calculations of effective  
13 rate constants in the supporting information has been mentioned and organized as “the effective  
14 rate constants for two bimolecular reactions of  $\text{H}_2\text{SO}_4 \cdots \text{H}_2\text{O} + \text{SO}_3$  and  $\text{SO}_3 \cdots \text{H}_2\text{O} + \text{H}_2\text{SO}_4$  were  
15 calculated, and the details were shown in *SI Appendix, Part 3 and Table 1*.”

16

17 **Comment 2.**

18 **Line 48:** “As a typical inorganic acid, SA can act as an important role in the new particle  
19 formation ...”

20 What is meant by “typical here? Please rephrase this sentence.

21 **Response:** Thanks for your valuable comments. It has been reported that  $\text{H}_2\text{SO}_4$  is a major  
22 inorganic acidic air pollutant (*Atmos. Chem. Phys.*, 2011, 11, 10803-10822.; *Atmos. Chem. Phys.*,  
23 2021, 21, 13483-13536.). So, according to the reviewer's suggestion, “As a typical inorganic acid,  
24 SA can act as an important role in the new particle formation...” has been changed as “As a major  
25 inorganic acidic air pollutant (Tilgner et al., 2021), SA can act as an important role in the new  
26 particle formation...”.

27

28 **Comment 3.**

29 **Line 82:** “It has been shown that the products of  $\text{SO}_3$  with some important atmospheric species  
30 have been identified in promoting NPF process.”

1 Such reaction would lead to the consumption of an SO<sub>3</sub> molecule potentially at the expense of  
2 forming less sulfuric acid. This competition should be further discussed in the manuscript.

3 **Response:** Thanks for your valuable comments. According to the reviewer's suggestion, the  
4 sentence of "It has been shown that the reaction between SO<sub>3</sub> and some important atmospheric  
5 species (Li et al., 2018a; Yang et al., 2021; Liu et al., 2019; Rong et al., 2020) not only can cause  
6 appreciable consumption of SO<sub>3</sub> and thus reduce the abundance of SA from the hydrolysis of SO<sub>3</sub>  
7 in the atmosphere, but also can promote NPF process by their products." has been added in Lines  
8 1-4 Page 4 of the revised manuscript. Moreover, to study the atmospheric importance of the SO<sub>3</sub> +  
9 H<sub>2</sub>SO<sub>4</sub> reaction without and with H<sub>2</sub>O, the rate ratio ( $v_{\text{DSA}}/v_{\text{SA}}$ ) between the SO<sub>3</sub> + H<sub>2</sub>SO<sub>4</sub> reaction  
10 and H<sub>2</sub>O-assisted hydrolysis of SO<sub>3</sub> was compared which has been organized in Lines 13-29 Page  
11 13 to Lines 1-11 Page 14.

#### 13 **Comment 4.**

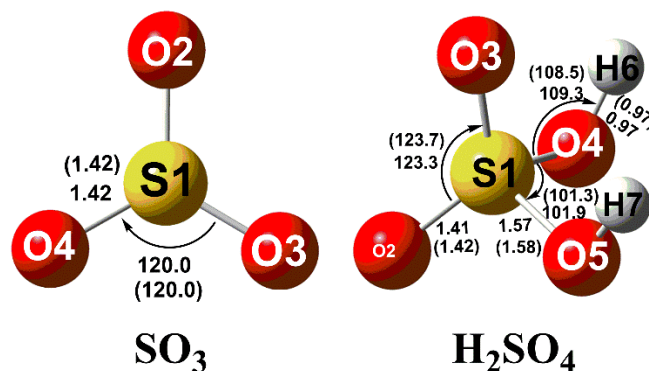
14 **Line 104:** I am missing some justification to why the M06-2X functional has been used and why  
15 the 6-311++G(2df,2pd) basis set was chosen. In addition, the M06-2X reference is incorrect.

16 **Response:** Thanks for your valuable comments. According to the reviewer's suggestion, the  
17 reason that M06-2X method with 6-311++G(2df,2pd) basis set has been added as follows.

18 (a) It has been proved that M06-2X functional is one of the best functionals to describe the  
19 noncovalent interactions and estimate the thermochemistry and equilibrium structures for  
20 atmospheric reactions. In Lines 22-24 Page 4 of the revised manuscript, the sentence of "The  
21 M06-2X functional has been proved to be one of the best functionals to describe the noncovalent  
22 interactions and estimate the thermochemistry and equilibrium structures for atmospheric  
23 reactions." has been added.

24 (b) The geometric parameters of the SO<sub>3</sub> and H<sub>2</sub>SO<sub>4</sub> reactants calculated at the M06-2X/6-  
25 311++G(3df,2pd) level have been shown in Fig. S1. As seen in Fig. S1, the mean absolute  
26 deviation of calculated bond distances and bond angles between the M06-2X/6-311++G(3df,2pd)  
27 level and the experimental reports were 0.005 Å and 0.45°, respectively. This reveals that the  
28 calculated bond distances and bond angles at the M06-2X/6-311++G(3df,2pd) level agree well  
29 with the available experimental values. So, the method of M06-2X/6-311++G(3df,2pd) was  
30 reliable to optimize the geometries of all the stationary points in the SO<sub>3</sub> + H<sub>2</sub>SO<sub>4</sub> reaction without

1 and with H<sub>2</sub>O. The corresponding details revision have been shown in Fig. S1. Thus, in Lines 1-2  
2 Page 4 of the revised manuscript, the sentence of “It is noted that the calculated bond distances  
3 and bond angles at the M06-2X/6-311++G(3df,2pd) level (Fig. S1) agree well with the available  
4 experimental values.” has been added.



5  
6 **Fig. R1** The optimized geometrical structures for the species of the SO<sub>3</sub> and HCl at M06-2X/6-  
7 311++G(3df,2pd) level of theory. The values in parentheses are the experimental values. Bond  
8 length is in angstrom and angle is in degree.

9 (c) As for M06-2X method, the correct references have been recited which has been  
10 organized as references (Zhao and Truhlar, 2008; Elm et al., 2012).

11 [1] Zhao, Y., and Truhlar, D. G.: The M06 suite of density functionals for main group  
12 thermochemistry, thermochemical kinetics, noncovalent interactions, excited states, and transition  
13 elements: two new functionals and systematic testing of four M06-class functionals and 12 other  
14 functionals, *Theor. Chem. Acc.*, 120, 215-241, 2008.;

15 [2] Elm, J., Bilde, M., and Mikkelsen, K. V.: Assessment of density functional theory in  
16 predicting structures and free energies of reaction of atmospheric pre-nucleation clusters, *J. Chem.*  
17 *Theory Comput.*, 8, 2071-2077, 2012.

18

19 **Comment 5.**

20 **Line 108:** The ORCA reference is incorrect.

21 **Response:** Thanks for your valuable comments. We are very sorry for using wrong references for  
22 the ORCA program. As for ORCA program, the corresponding reference have been recited and  
23 organized as references (Neese, 2012).

24 [1] Neese, F.: The ORCA program system, *WIREs Comput. Mol. Sci.*, 2, 73-78,  
25 <https://doi.org/10.1002/wcms.81>, 2012.

1

2 **Comment 6.**

3 **Line 110-116:** I am in doubt whether the applied configurational sampling of the clusters is  
4 sufficient to identify the lowest free energy cluster structures. Only calculating 1000 local minima  
5 from the ABCcluster search sounds a bit low on the low side. How certain are the authors that they  
6 have located the global minimum? As the CHARMM forcefield cannot handle bond breaking a  
7 more diverse pool of clusters is needed. This is usually done by performing ABCcluster runs with  
8 ionic monomers as well (see Kubečka et al., <https://doi.org/10.1021/acs.jpca.9b03853>). Only  
9 selecting the lowest 100 cluster configurations based on PM6 could lead to the global minimum  
10 cluster being missed (see Kurfman et al., <https://doi.org/10.1021/acs.jpca.1c00872>).

11 **Response:** Thanks for your valuable comments. We are very sorry for missing a ‘*n*’ for the  
12 configurational sampling method. Indeed, a multi-path searching approach is adopted in this work,  
13 which expands the search range. As for every global minimum cluster, *n* kinds of searching  
14 pathways have been considered, and 1000 autogenerated structures in every searching pathway  
15 were first carried out using ABCcluster software, and were optimized at the semi-empirical PM6  
16 methods using MOPAC 2016. Then, up to *n*\*100 structures with relatively lowest energy among  
17 the *n*\*1000 ( $1 < n < 5$ ) structures were selected and reoptimized at the M06-2X/6-31+G(*d,p*) level.  
18 Finally, *n*\*10 lowest-lying structures were optimized by the M06-2X/6-311++G(2*df*,2*pd*) level to  
19 determine the global minimum. So, the method for configurational sampling of the clusters has  
20 been corrected as “Specifically, a multistep global minimum sampling technique was used to  
21 search for the global minima of the (SA)<sub>*x*</sub>(A)<sub>*y*</sub>(DSA)<sub>*z*</sub> ( $0 < y \leq x + z \leq 3$ ) clusters. Specifically, the  
22 initial *n*\*1000 ( $1 < n < 5$ ) configurations for each cluster were systematically generated by the  
23 ABCcluster program (Zhang and Dolg, 2015), and were optimized at the semi-empirical PM6  
24 (Stewart, 2013) methods using MOPAC 2016 (Stewart, 2013; Stewart, 2007). Then, up to *n*\*100  
25 structures with relatively lowest energy among the *n*\*1000 ( $1 < n < 5$ ) structures were selected and  
26 reoptimized at the M06-2X/6-31+G(*d,p*) level. Finally, *n*\*10 lowest-lying structures were  
27 optimized by the M06-2X/6-311++G(2*df*,2*pd*) level to determine the global minimum. The  
28 optimized structures and the formation Gibbs free energy of the stable clusters were summarized  
29 in Fig. S9 and Table S8 of the SI Appendix, respectively.” in Line 8-19 Page 5 of the revised  
30 manuscript.

1

2 **Comment 7.**

3 **Line 116:** Here it is stated that the free energies are calculated at the M06-2X/6-311++G(2df,2pd)  
4 level of theory. However, Table S8 indicates that DLPNO-CCSD(T) single point energy  
5 calculations were carried out on top of the clusters.

6 **Response:** Thanks for your valuable comments. We apologize for the reviewer's  
7 misunderstanding of the calculation methodology. Indeed, the M06-2X/6-311++G(2df,2pd)  
8 method has been used to optimize the geometries of (DSA)<sub>x</sub>(SA)<sub>y</sub>(A)<sub>z</sub> ( $z \leq x + y \leq 3$ ) molecular  
9 clusters, while the single-point energy calculations were refined at the DLPNO-CCSD(T)/aug-cc-  
10 pVTZ level based on the optimized geometries at the M06-2X/6-311++G(2df,2pd) level. In order  
11 to express the calculated method clearly, in Lines 16-18 Page 5 of the revised manuscript, the  
12 sentence of "To obtain the reliable energies, single-point energy calculations were refined at the  
13 DLPNO-CCSD(T)/aug-cc-pVTZ level based on the optimized geometries at the M06-2X/6-  
14 311++G(2df,2pd) level" has been added.

15

16 **Comment 8.**

17 **Line 147:** How was the 191 water cluster obtained? Has this cluster been equilibrated before the  
18 SO<sub>3</sub> and H<sub>2</sub>SO<sub>4</sub> was added? Or after? Some more details about how the system was setup is  
19 needed. Is a 1 fs timestep adequate to capture the desired dynamics? I.e. can it actually capture the  
20 hydrogen bond stretching vibration?

21 **Response:** Thanks for your valuable comments. According to the reviewer's suggestion, the  
22 reason for selecting the droplet system with 191 water molecules has been explained firstly.  
23 Meanwhile, it is pointed out that the droplet system with 191 water molecules has been  
24 equilibrated before SO<sub>3</sub> and H<sub>2</sub>SO<sub>4</sub> was added at the water surface. Finally, the reason for setting a  
25 1 fs timestep in the dynamic simulations has been explained. The corresponding revision has been  
26 respectively made as follows.

27 (a) The size effect on interfacial mechanism has been reported by Zhong et al. (*J. Am. Chem.*  
28 *Soc.*, 2017, 139, 47, 17168-17174), where the behavior of SO<sub>2</sub> adsorption on droplet with 24, 48,  
29 96 and 191 water molecules has been studied. The work reported by Zhong et al. (*J. Am. Chem.*  
30 *Soc.*, 2017, 139, 47, 17168-17174) shows that the smaller droplet is subjected to large deformation



1 during the system evolution, and the droplet system with 191 water molecules are sufficient to  
2 describe the interfacial mechanism. So, we only consider the droplet system with 191 water  
3 molecules in the BOMD simulation. The radius of the water droplet in our system was  
4 approximately 10.7 Å and a cubic simulation box of side 35 Å was used. The similar set of  
5 simulation box have been found widely in previous works. (*J. Am. Chem. Soc.*, 2016, 138, 1816-  
6 1819; *Proc. Natl. Acad. Sci. U.S.A.*, 2017, 114, 12401-12406.; *J. Am. Chem. Soc.*, 2018, 140, 6456-  
7 6466.; *J. Am. Chem. Soc.*, 2018, 140, 14, 4913-4921.; *Chem. Sci.*, 2019, 10, 743-751.; *Chem. Sci.*,  
8 2017,8, 5385-5391.). So, in Lines 20-22 Page 6 of the revised manuscript, the droplet system with  
9 191 water molecules has been reorganized as “As the droplet system with 191 water molecules are  
10 sufficient to describe the interfacial mechanism, the air-water interfacial system here included 191  
11 water molecules, SO<sub>3</sub> and SA in the BOMD simulation.”.

12 (b) The droplet system with 191 water molecules has been equilibrated before SO<sub>3</sub> and  
13 H<sub>2</sub>SO<sub>4</sub> was added at the water surface. Specifically, a nearly spherical droplet with 191 water  
14 molecules was firstly constructed by using the Packmol program (*J. Comput. Chem.*, 2009, 30,  
15 2157-2164.) with a tolerance of 2.0 Å, namely, all atoms from different molecules will be at least  
16 2.0 Å apart. Then, based on the resulting initial structure, the GROMACS software (*J. Comput.*  
17 *Chem.*, 2005, 26, 1701-1718.) with the general AMBER force field (GAFF) (*J. Comput. Chem.*  
18 2004, 25, 1157-1174.) was used to simulate the droplet equilibrium process with two steps. In the  
19 first step, a water slab of 35 × 35 × 35 Å<sup>3</sup> containing 191 water molecules was built using periodic  
20 boundary conditions to avoid the effect of neighboring replicas. In the second step, the water slab  
21 was fully equilibrated for 1 ns under NVT ensemble (N, V and T represent the number of atoms,  
22 volume and temperature, respectively) to reach equilibrium state. The water molecules were  
23 described by the TIP3P model. The isothermal-isochoric (NVT) simulation was executed at 298 K  
24 for simulation system. The temperature was kept constant by the V-rescale thermostat coupling  
25 algorithm. The coupling time constant is 0.1 ps. Bond lengths were constrained by the LINCS  
26 algorithm. The cut-off distance of 1.2 nm was set for van der Waals (vdW) interactions. The  
27 Particle Mesh Ewald (PME) summation method was used to calculate the electrostatic interactions.  
28 During the whole simulation process, a time step of 2 fs was set and three-dimensional periodic  
29 boundary conditions were adopted. Next, to ensure the stability of the system, the droplets were  
30 pre-optimized using BOMD at 300 K for 10 ps prior to the simulation of the air-water interfacial

1 reaction. Using the density functional theory (DFT) method, the electronic exchange-correlation  
2 term was described by the Becke-Lee-Yang-Parr (BLYP) functional. The Grimme's dispersion  
3 correction (D3) was applied to account for the weak dispersion interaction. The double- $\zeta$  Gaussian  
4 (DZVP-MOLOPT) basis set and the Goedecker-Teter-Hutter (GTH) norm-conserving  
5 pseudopotentials were adopted to treat the valence and the core electrons, respectively. The  
6 planewave cutoff energy is set to 280 Ry, and that for the Gaussian basis set is 40 Ry. And the  
7 SCF convergence criterion is 1.0E-5 Hartree. All simulations were performed in NVT ensemble  
8 with Nose-Hoover thermostat controlling the temperature. Finally, the SO<sub>3</sub> and H<sub>2</sub>SO<sub>4</sub> molecule  
9 was added at the water surface after the droplet system with 191 water molecules was fully  
10 equilibrated. The details of the equilibrium process for the droplet system with 191 water  
11 molecules are shown in the *SI Appendix* Part 4. Meanwhile, the sentence of “It is pointed out that  
12 the droplet system with 191 water molecules has been equilibrated before SO<sub>3</sub> and H<sub>2</sub>SO<sub>4</sub> was  
13 added at the water surface. The details of the equilibrium process for the droplet system with 191  
14 water molecules are shown in the *SI Appendix* Part 4.” has been added in Lines 22-25 Page 6 of  
15 the revised manuscript.

16 (c) In the interfacial BOMD simulations, the timestep was set to be 1.0 fs, as it has been  
17 proved to achieve sufficient energy conservation for the water system (*J. Chem. Theory Comput.*,  
18 2011, 7, 2937-2946.; *J. Am. Chem. Soc.* 2015, 137, 12070.; *J. Am. Chem. Soc.* 2016, 138, 1816.; *J.*  
19 *Am. Chem. Soc.* 2016, 138, 11164.; *Chem. Sci.* 2017, 8, 5385.). So, the sentence of “Notably, the  
20 timestep of 1.0 fs has been proved to achieve sufficient energy conservation for the water system.”  
21 has been added in Lines 27-28 Page 6 of revised manuscript.

22

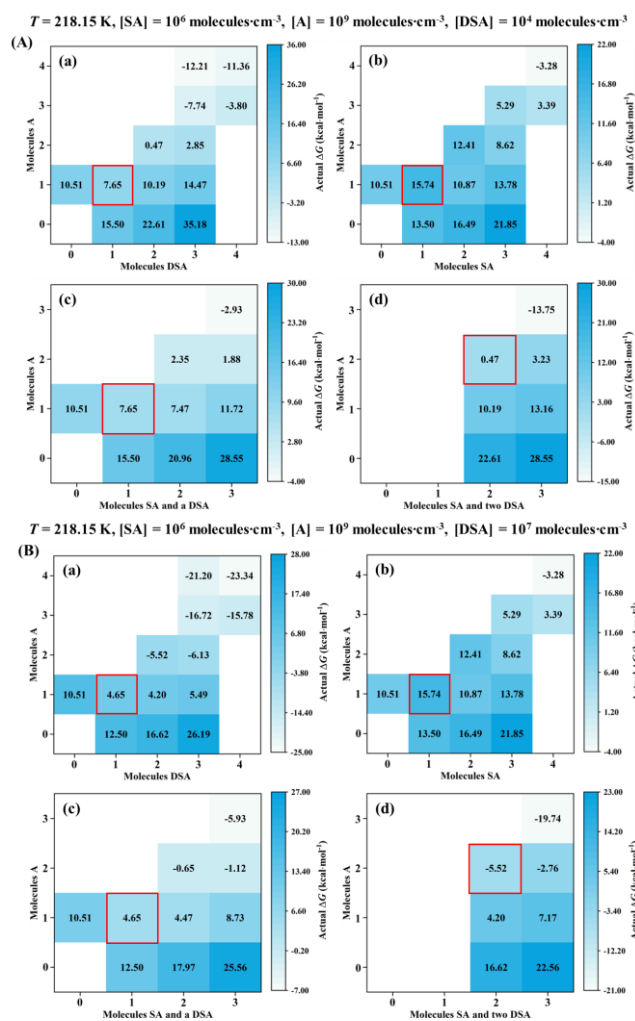
### 23 **Comment 9.**

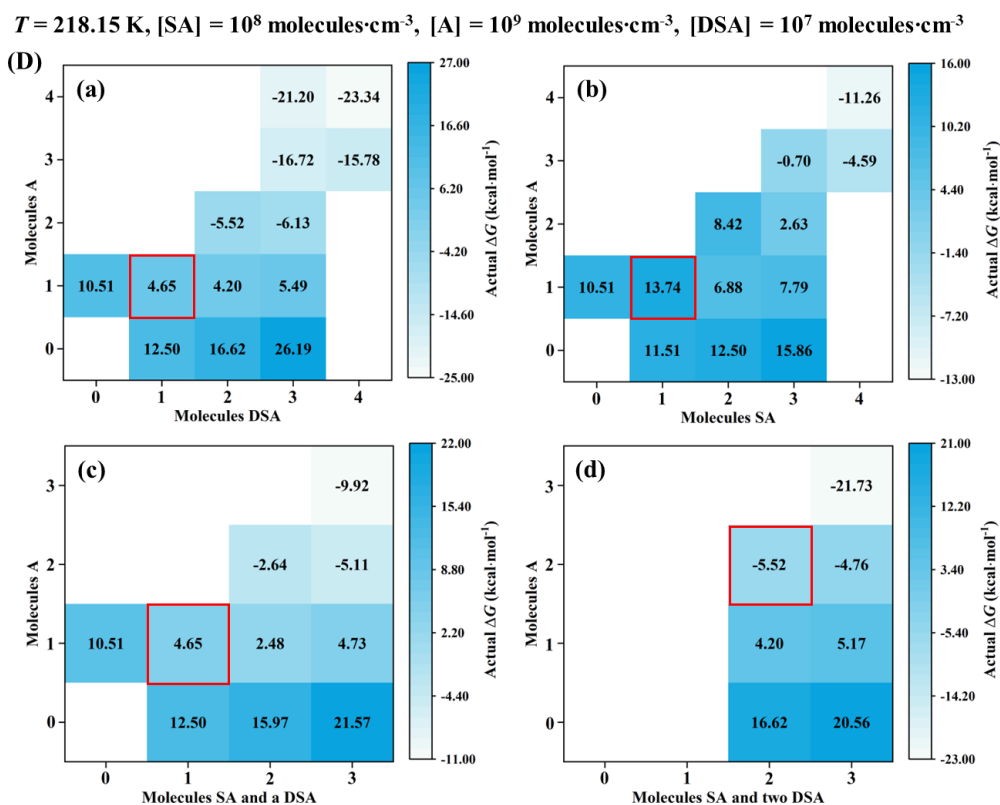
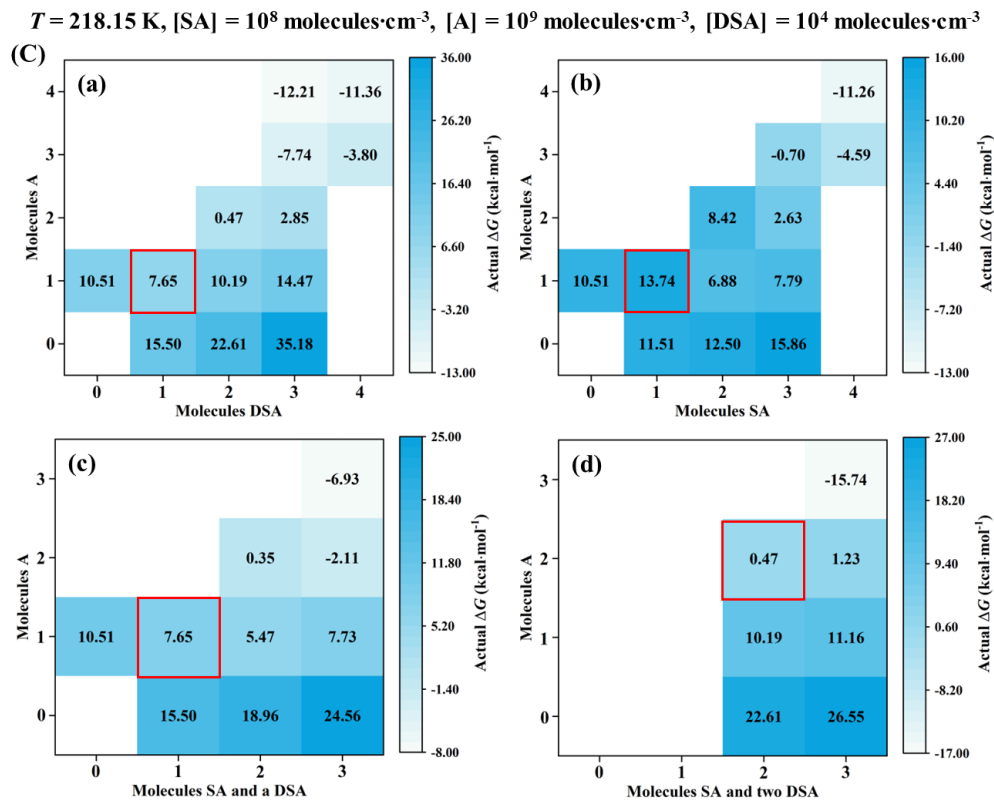
24 **Line 156:** I am not entirely convinced that the 3 × 3 system “box” size is large enough to ensure  
25 meaningful cluster dynamics of the systems. For instance, the work by Besel et al.  
26 (<https://doi.org/10.1021/acs.jpca.0c03984>) showed how the sulfuric acid-ammonia system is  
27 impacted by the studied box size. Please elaborate on this aspect.

28 Also is the sulfur concentration constrained in the simulations? A single DSA molecule would  
29 consume 2 sulfuric acids. 1 SA and 1 SO<sub>3</sub> that could form SA. Hence, the simulations might  
30 actually “push” additional sulfur into the system.

1 **Response:** Thanks for your valuable comments. For reviewers' comments, the corresponding  
 2 revision has been respectively made as follows.

3 (a) As the work reported by Besel et al. (*J. Phys. Chem. A*, **2020**, 124(28), 5931-5943), the  
 4 explicitly simulated set of clusters should always include the “critical cluster”. Also, the highest  
 5 barrier on the lowest-energy path connecting the monomers to the outgrowing clusters (a saddle  
 6 point on the actual  $\Delta G$  surface) represents the “critical cluster”. So, at 218.15 K (Fig. S12) and  
 7 238.15 K (Fig. S13), the actual  $\Delta G$  of  $(A)_y(DSA)_z$  ( $0 \leq y \leq z \leq 4$ ),  $(SA)_x(A)_y$  ( $0 \leq y \leq x \leq 4$ ),  
 8  $(SA)_x(A)_y(DSA)_1$  ( $0 \leq y \leq 3, 0 \leq x \leq 2$ ), and  $(SA)_x(A)_y(DSA)_2$  ( $0 \leq y \leq 3, 0 \leq x \leq 1$ ) clusters has  
 9 been calculated to ensure meaningful cluster dynamics of the  $3 \times 3$  systems. As seen in Fig. S12  
 10 and S13, the actual  $\Delta G$  surface represented that the simulated set of clusters always included the  
 11 critical cluster. So, we conclude that, in atmospherically relevant conditions, a  $3 \times 3$  cluster set is  
 12 adequate for predicting the particle formation in the SA-A system.

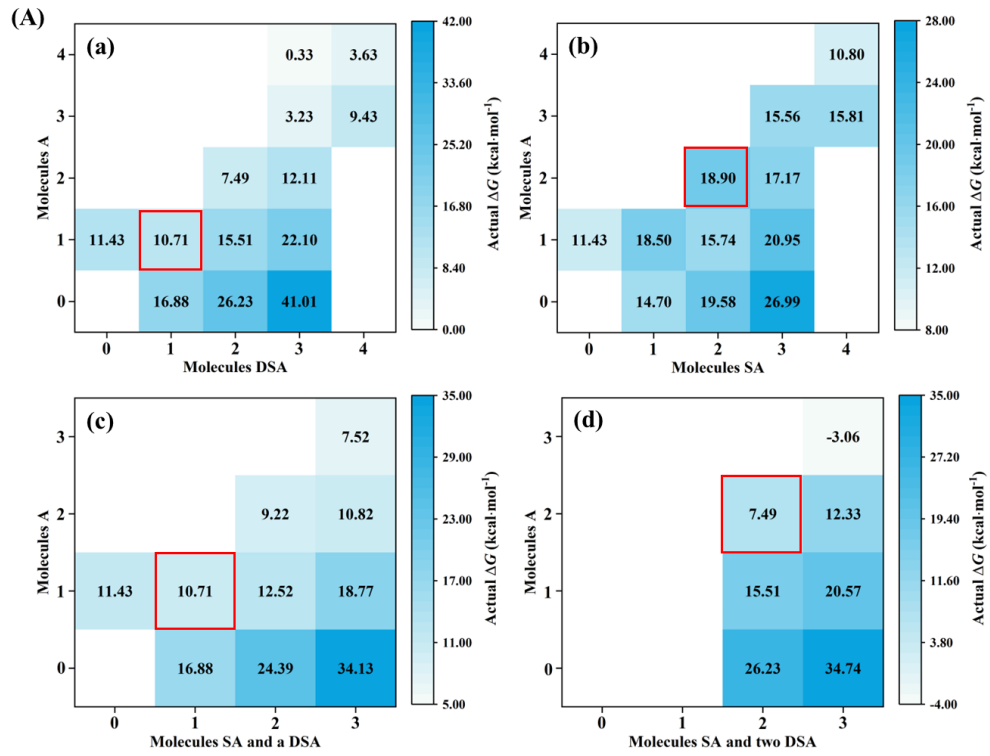




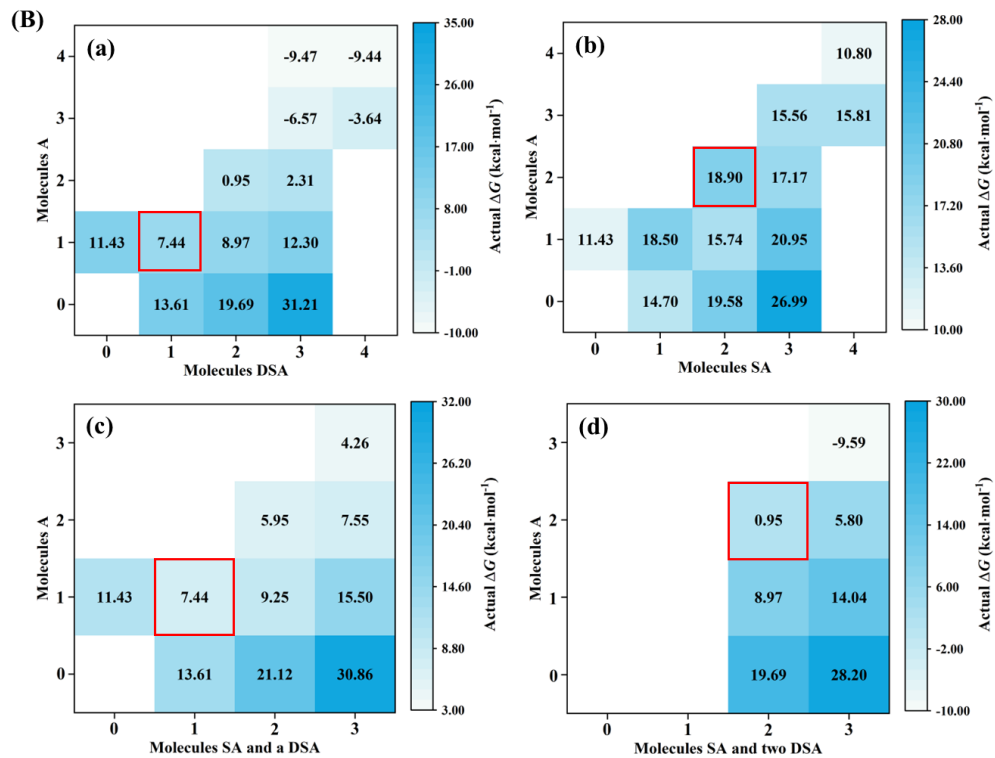
1  
2  
3

**Fig. S12** A typical actual  $\Delta G$  surface at 218.15 K.  $[\text{SA}]$  is the concentration of sulfuric acid monomers,  $[\text{A}]$  the concentration of ammonia monomers and  $[\text{DSA}]$  is disulfuric acid

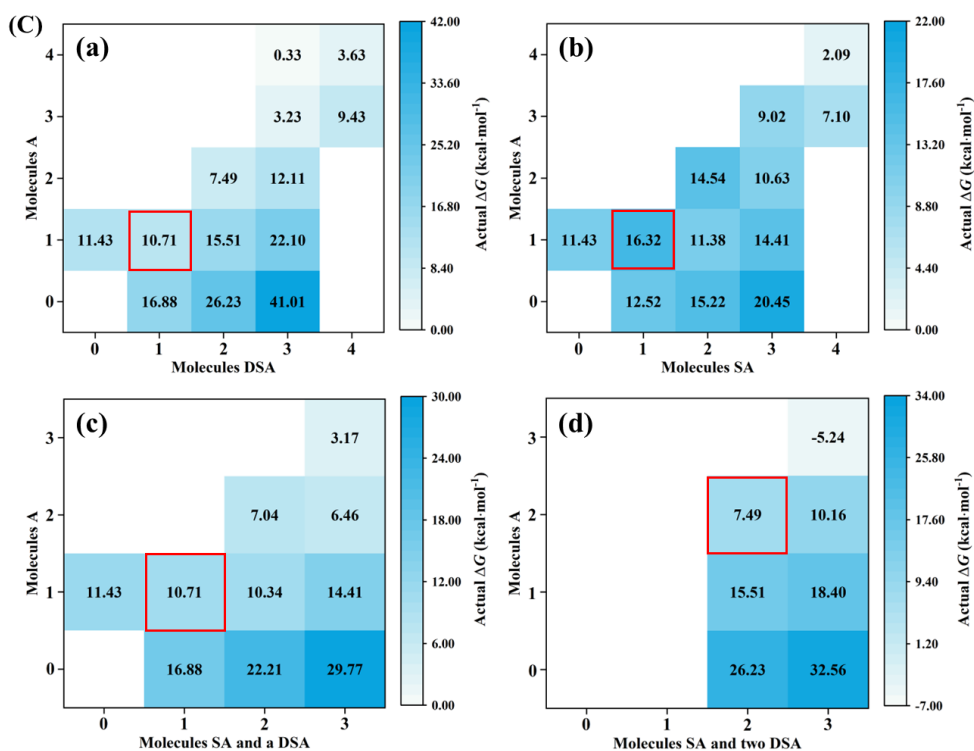
$T = 238.15 \text{ K}$ ,  $[\text{SA}] = 10^6 \text{ molecules}\cdot\text{cm}^{-3}$ ,  $[\text{A}] = 10^9 \text{ molecules}\cdot\text{cm}^{-3}$ ,  $[\text{DSA}] = 10^4 \text{ molecules}\cdot\text{cm}^{-3}$



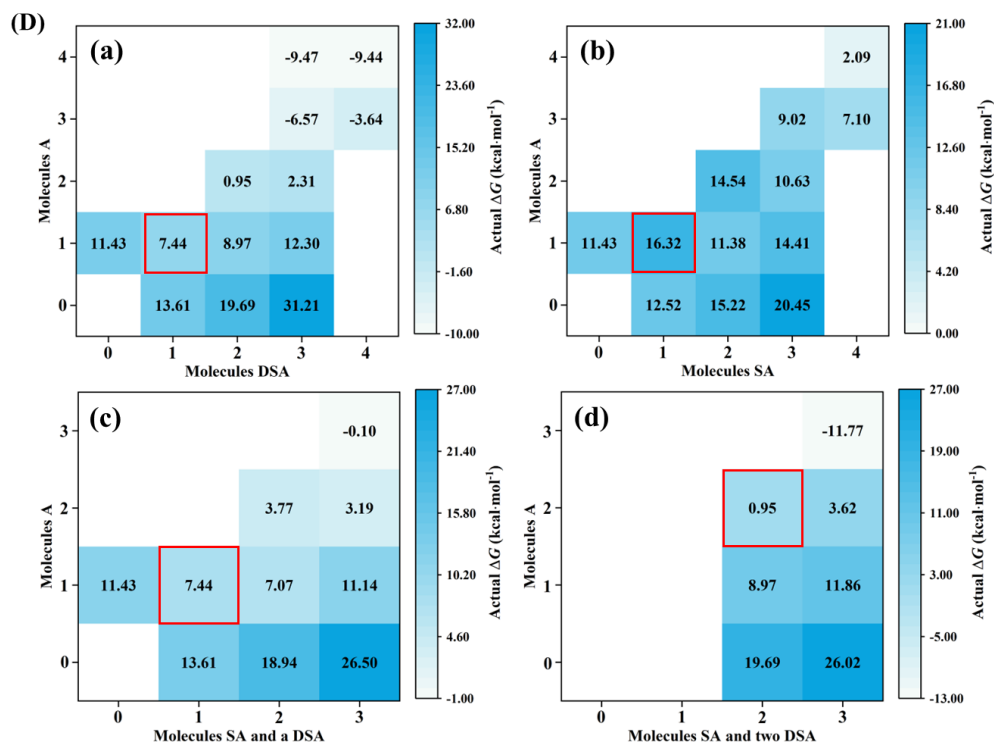
$T = 238.15 \text{ K}$ ,  $[\text{SA}] = 10^6 \text{ molecules}\cdot\text{cm}^{-3}$ ,  $[\text{A}] = 10^9 \text{ molecules}\cdot\text{cm}^{-3}$ ,  $[\text{DSA}] = 10^7 \text{ molecules}\cdot\text{cm}^{-3}$



$T = 238.15 \text{ K}$ ,  $[\text{SA}] = 10^8 \text{ molecules}\cdot\text{cm}^{-3}$ ,  $[\text{A}] = 10^9 \text{ molecules}\cdot\text{cm}^{-3}$ ,  $[\text{DSA}] = 10^4 \text{ molecules}\cdot\text{cm}^{-3}$



$T = 238.15 \text{ K}$ ,  $[\text{SA}] = 10^8 \text{ molecules}\cdot\text{cm}^{-3}$ ,  $[\text{A}] = 10^9 \text{ molecules}\cdot\text{cm}^{-3}$ ,  $[\text{DSA}] = 10^7 \text{ molecules}\cdot\text{cm}^{-3}$

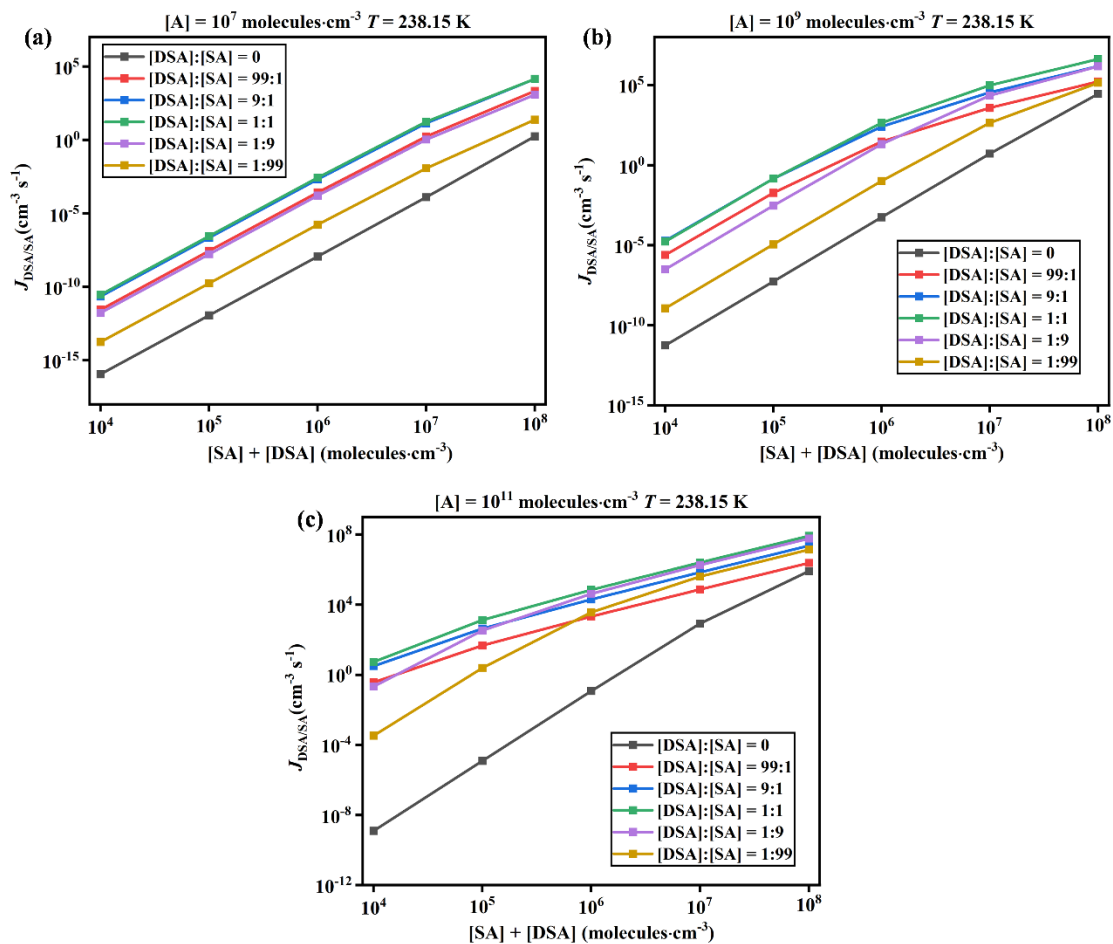


1

2 **Fig. S13** A typical actual  $\Delta G$  surface at 238.15 K.  $[\text{SA}]$  is the concentration of sulfuric acid  
 3 monomers,  $[\text{A}]$  the concentration of ammonia monomers and  $[\text{DSA}]$  is disulfuric acid

4 (b) As mentioned by the reviewer, each DSA molecule generated consumes one SA molecule,  
 5 resulting the simulations might “push” additional sulfur into the system. So, when the sum ( $[\text{SA}] +$

1 [DSA]) is kept constant ( $10^4 - 10^8$  molecules·cm<sup>-3</sup>), Fig. S19 shows particle formation rates ( $J$ , cm<sup>-3</sup>·s<sup>-1</sup>) with varying ratios of [DSA]:[SA] at 238.15 K under different A concentrations ((a) $10^7$  molecules·cm<sup>-3</sup>, (b) $10^9$  molecules·cm<sup>-3</sup>, (c) $10^{11}$  molecules·cm<sup>-3</sup>).



4  
5 **Fig. S19** Particle formation rates ( $J$ , cm<sup>-3</sup>·s<sup>-1</sup>) with varying ratios of [DSA]:[SA] at 238.15 K  
6 under different A concentrations ((a) $10^7$  molecules·cm<sup>-3</sup>, (b) $10^9$  molecules·cm<sup>-3</sup>, (c) $10^{11}$   
7 molecules·cm<sup>-3</sup>). [DSA] + [SA] =  $10^4$ - $10^8$  molecules·cm<sup>-3</sup>

8 As shown in Fig. S19(a), at lower atmospheric concentration of A ( $10^7$  molecules·cm<sup>-3</sup>), the  
9 formation rate  $J_{\text{DSA/SA}}$  at 1% substitution ([DSA]:[SA] = 1:99) was higher than that at  
10 unsubstituted condition ([DSA]:[SA] = 0:100). Similarly,  $J_{\text{DSA/SA}}$  at 10% substitution ([DSA]:[SA]  
11 = 1:9) was higher than that at 1% substitution. Moreover,  $J_{\text{DSA/SA}}$  at 50% substitution ([DSA]:[SA]  
12 = 1:1) reach a maximum value ( $1.41 \times 10^4$  cm<sup>-3</sup>·s<sup>-1</sup>), which is larger by 4-5 orders of magnitude  
13 than the value at unsubstituted condition. These results at lower atmospheric concentration of A  
14 show that the enhancement strength of DSA on the particle formation rate of SA-A-based clusters  
15 increases with the increasing of the percentage of substitution.

16 At medium ( $10^9$  molecules·cm<sup>-3</sup>) and higher ( $10^{11}$  molecules·cm<sup>-3</sup>) atmospheric concentration

1 of A,  $J_{\text{DSA/SA}}$  at 50% substitution ( $[\text{DSA}]:[\text{SA}] = 1:1$ ) reaches a maximum value. As compared  
2 with  $J_{\text{DSA/SA}}$  at unsubstituted condition, the value of  $J_{\text{DSA/SA}}$  at 50% substitution ( $[\text{DSA}]:[\text{SA}] = 1:1$ )  
3 enhanced by 10 and 11 orders of magnitude, respectively. However, as the percentage of  
4 substitution ( $> 50\%$ ) increases, the value of  $J_{\text{DSA/SA}}$  at medium and higher  $[\text{A}]$  decreases. This may  
5 be due to the fact that in the pure A-DSA nucleation system, large stable clusters  $(\text{A})_3 \cdot (\text{DSA})_3$  can  
6 only be formed by mutual collisions of  $\text{A} \cdot \text{DSA}$  clusters. So, DSA has the same “acid” molecular  
7 properties as SA in the SA-A-DSA ternary nucleation system. We predicted that DSA is a  
8 relatively stronger nucleation precursor than SA.

9 Besides, it should be noted that the concentration of water in the troposphere is abundant, and  
10 DSA is easily hydrolyzed to form 2  $\text{H}_2\text{SO}_4$  molecules. Based on this, the concentration of DSA  
11 listed in Fig. S9 was overestimated. However, the extent and proportion of DSA hydrolysis  
12 remains unclear, and the hydrolysis behavior of DSA needs to be further investigated in  
13 subsequent studies. Therefore, the maximum concentration of DSA ( $10^8 \text{ molecules} \cdot \text{cm}^{-3}$ ) was not  
14 included in the effect of  $\text{H}_2\text{S}_2\text{O}_7$ , the product of the reaction between  $\text{SO}_3$  and  $\text{H}_2\text{SO}_4$ , on new  
15 particle formation (NPF) in various environments by using the Atmospheric Cluster Dynamics  
16 Code kinetic model and the QC calculation. In Lines 27-29 Page 7 to Lines 1-2 Page 7 of the  
17 revised manuscript, the discussion of the DSA concentration has been added as “As the prediction  
18 in Table S7, the concentration of DSA is set to  $10^4$ - $10^8 \text{ molecules} \cdot \text{cm}^{-3}$ . However, DSA is easily  
19 hydrolyzed with abundant water in the troposphere to form  $\text{H}_2\text{SO}_4$ , the concentration of DSA  
20 listed in Fig. S9 was overestimated. So, the maximum concentration of DSA ( $10^8 \text{ molecules} \cdot \text{cm}^{-3}$ )  
21 was not included in the effect of  $\text{H}_2\text{S}_2\text{O}_7$  on new particle formation (NPF) in various  
22 environments.”

23

#### 24 **Comment 10.**

25 **Line 162:** I do not believe the factors of 1/2 should be in this equation.

26 **Response:** Thanks for your valuable comments. The equation has been checked carefully and the  
27 equation is correct. This is consistent with the previous literature (*Chemosphere*, **2020**, 245,  
28 125554.; **2018**, 203, 26-33.; *Phys. Chem. Chem. Phys.*, **2018**, 20, 17406-17414.; **2023**, 25, 16745.;  
29 *Atmos. Chem. Phys.*, **2012**, 12, 2345-2355.; **2022**, 22, 2639-2650.; **2021**, 21, 6221-6230.; **2022**,  
30 22, 1951-1963.; *J. Chem. Phys.*, **2017**, 146, 184308.)



1 **Comment 11.**

2 **Line 168-169:** Please explicitly mention the boundary conditions and concentration ranges in the  
3 text here instead of referring to the SI.

4 **Response:** Thank you for your valuable comments. According to your suggestion, boundary  
5 conditions and concentration ranges have been added in Lines 20-29 Page 7 to Lines 1-4 Page 8 of  
6 the revised manuscript, which has been organized as “**The boundary conditions in the ACDC**  
7 **require that the smallest clusters outside of the simulated system should be very stable so that not**  
8 **to evaporate back immediately (McGrath et al., 2012). Based on cluster volatilization rate (shown**  
9 **in Table S10) and the formation Gibbs free energy of the clusters (shown in Table S8), the cluster**  
10 **boundary conditions simulated in this study were set as (SA)<sub>4</sub>·(A)<sub>3</sub>, (SA)<sub>4</sub>·(A)<sub>4</sub>, SA·(A)<sub>3</sub>·(DSA)<sub>3</sub>,**  
11 **(SA)<sub>3</sub>·(A)<sub>4</sub>·(DSA)<sub>1</sub> and (SA)<sub>2</sub>·(A)<sub>3</sub>·(DSA)<sub>2</sub>. According to field observations, the concentration of**  
12 **SA and A was respectively set in a range of 10<sup>6</sup>-10<sup>8</sup> molecules·cm<sup>-3</sup> and 10<sup>7</sup>-10<sup>11</sup> molecules·cm<sup>-3</sup>**  
13 **(Almeida et al., 2013; Kuang et al., 2008; Bouo et al., 2011; Zhang et al., 2018). As the prediction**  
14 **in Table S7, the concentration of DSA is set to 10<sup>4</sup>-10<sup>8</sup> molecules·cm<sup>-3</sup>. However, DSA is easily**  
15 **hydrolyzed with abundant water in the troposphere to form H<sub>2</sub>SO<sub>4</sub>, the concentration of DSA**  
16 **listed in Fig. S9 was overestimated. So, the maximum concentration of DSA (10<sup>8</sup> molecules·cm<sup>-3</sup>)**  
17 **was not included in the effect of H<sub>2</sub>S<sub>2</sub>O<sub>7</sub> on new particle formation (NPF) in various environments.**  
18 **Besides, the temperature was set to be 218.15-298.15 K, which span most regions of the**  
19 **troposphere and the polluted atmospheric boundary layer.”**

20

21 **Comment 12.**

22 **Section 3.1:** I am missing some comments on why the titled reaction is of interest and how much  
23 the competitive pathway of SO<sub>3</sub> + H<sub>2</sub>O matters. Would SO<sub>3</sub> not react with water instead of H<sub>2</sub>SO<sub>4</sub>?  
24 What are the branching ratios between these reaction pathways?

25 **Response:** Thanks for your valuable comments. The reason for our interest in SO<sub>3</sub> + H<sub>2</sub>SO<sub>4</sub>  
26 reaction and the importance of the competition between the SO<sub>3</sub> + H<sub>2</sub>SO<sub>4</sub> reaction and H<sub>2</sub>O-  
27 assisted hydrolysis of SO<sub>3</sub> have been discussed. The corresponding major revision has been made  
28 as follows.

29 (a) Sulfur trioxide (SO<sub>3</sub>) is a major air pollutant and can be considered as the most  
30 important oxidation product of SO<sub>2</sub>. As an active atmospheric species, SO<sub>3</sub> can lead to the

1 formations of acid rain and atmospheric aerosol and thus plays a well-documented role in regional  
 2 climate and human health. In the atmosphere, the hydrolysis of SO<sub>3</sub> to product H<sub>2</sub>SO<sub>4</sub> is the most  
 3 major loss route of SO<sub>3</sub>. Meanwhile, SO<sub>3</sub> can also react with NH<sub>3</sub>, CH<sub>3</sub>OH, HNO<sub>3</sub>, HCl, organic  
 4 acids (such as HCOOH), et al. the products of SO<sub>3</sub> with some important atmospheric species have  
 5 been identified in promoting NPF process. However, H<sub>2</sub>SO<sub>4</sub> plays a significant role as a major  
 6 inorganic acidic air pollutant in the new particle formation and acid rain. The reaction of SO<sub>3</sub> with  
 7 H<sub>2</sub>SO<sub>4</sub> has not been investigated as far as we know. Thus, it is important to study the mechanism  
 8 between SO<sub>3</sub> and H<sub>2</sub>SO<sub>4</sub>.

9 (b) To understand the competition between the SO<sub>3</sub> + H<sub>2</sub>SO<sub>4</sub> reaction and H<sub>2</sub>O-assisted  
 10 hydrolysis of SO<sub>3</sub> in the Earth's atmosphere, the rate ratio ( $v_{\text{DSA}}/v_{\text{SA}}$ ) between the SO<sub>3</sub> + H<sub>2</sub>SO<sub>4</sub>  
 11 reaction and H<sub>2</sub>O-assisted hydrolysis of SO<sub>3</sub> has been calculated and was expressed in Eq. (4).

$$12 \quad \frac{v_{\text{DSA}}}{v_{\text{SA}}} = \frac{k_{\text{DSA}} \times [\text{SO}_3] \times [\text{H}_2\text{SO}_4] + k_{\text{DSA\_WM}_s} \times K_{\text{eq1}} \times [\text{SO}_3] \times [\text{H}_2\text{SO}_4] \times [\text{H}_2\text{O}]}{k_{\text{SA\_WM}} \times K_{\text{eq2}} \times [\text{SO}_3] \times [\text{H}_2\text{O}] \times [\text{H}_2\text{O}]} \quad (4)$$

13 In Eq. (4),  $K_{\text{eq1}}$  and  $K_{\text{eq2}}$  were the equilibrium constant for the formation of H<sub>2</sub>SO<sub>4</sub>···H<sub>2</sub>O and  
 14 SO<sub>3</sub>···H<sub>2</sub>O complexes shown in Table S2, respectively;  $k_{\text{DSA}}$ ,  $k_{\text{DSA\_WM}_s}$  and  $k_{\text{SA\_WM}}$  were  
 15 respectively denoted the bimolecular rate coefficient for the H<sub>2</sub>SO<sub>4</sub> + SO<sub>3</sub>, H<sub>2</sub>SO<sub>4</sub>···H<sub>2</sub>O + SO<sub>3</sub>  
 16 and SO<sub>3</sub>···H<sub>2</sub>O + H<sub>2</sub>O reactions; [H<sub>2</sub>O] and [H<sub>2</sub>SO<sub>4</sub>] were respectively represented the  
 17 concentration of H<sub>2</sub>O and H<sub>2</sub>SO<sub>4</sub> taken from references (*J. Phys. Chem. A*, 2013, 117, 10381-  
 18 10396.; *Environ. Sci. Technol.*, 2015, 49, 13112-13120.). The corresponding rate ratio have been  
 19 listed in Table S7 (0 km altitude) and S8 (5-30 km altitude). As seen in Table S7, at 0 km altitude,  
 20 the hydrolysis reaction of SO<sub>3</sub> with (H<sub>2</sub>O)<sub>2</sub> is more favorable than the SO<sub>3</sub> + H<sub>2</sub>SO<sub>4</sub> reaction as the  
 21 [H<sub>2</sub>O] (10<sup>16</sup>-10<sup>18</sup> molecules·cm<sup>3</sup>) is much larger than that of [H<sub>2</sub>SO<sub>4</sub>] (10<sup>4</sup>-10<sup>8</sup> molecules·cm<sup>3</sup>).  
 22 Although the concentration of water molecules decreases with the increase of altitude in Table S8,  
 23 the concentration of [H<sub>2</sub>O] is still much greater than that of [H<sub>2</sub>SO<sub>4</sub>], resulting in the SO<sub>3</sub> + H<sub>2</sub>SO<sub>4</sub>  
 24 reaction cannot compete with H<sub>2</sub>O-assisted hydrolysis of SO<sub>3</sub> within the altitude range of 5-30 km.  
 25 Moreover, the SO<sub>3</sub> + H<sub>2</sub>SO<sub>4</sub> reaction is not also the major sink route of SO<sub>3</sub>, even considering of  
 26 high H<sub>2</sub>SO<sub>4</sub> concentration at the end and outside the aircraft engine and flight. Based on this, the  
 27 sentence of “The value of  $v_{\text{DSA}}/v_{\text{SA}}$  was listed in Table S7 (0 km altitude) and S8 (5-30 km  
 28 altitude). As seen in Table S7, at 0 km altitude, the hydrolysis reaction of SO<sub>3</sub> with (H<sub>2</sub>O)<sub>2</sub> is more  
 29 favorable than the SO<sub>3</sub> + H<sub>2</sub>SO<sub>4</sub> reaction as the [H<sub>2</sub>O] (10<sup>16</sup>-10<sup>18</sup> molecules·cm<sup>3</sup>) is much larger

1 than that of [H<sub>2</sub>SO<sub>4</sub>] (10<sup>4</sup>-10<sup>8</sup> molecules·cm<sup>-3</sup>). Although the concentration of water molecules  
2 decreases with the increase of altitude in Table S8, the concentration of [H<sub>2</sub>O] is still much greater  
3 than that of [H<sub>2</sub>SO<sub>4</sub>], resulting in the SO<sub>3</sub> + H<sub>2</sub>SO<sub>4</sub> reaction cannot compete with H<sub>2</sub>O-assisted  
4 hydrolysis of SO<sub>3</sub> within the altitude range of 5-30 km. Even considering of high H<sub>2</sub>SO<sub>4</sub>  
5 concentration at the end and outside the aircraft engine and flight at 10 km (Curtius et al., 2002),  
6 the SO<sub>3</sub> + H<sub>2</sub>SO<sub>4</sub> reaction is not also the major sink route of SO<sub>3</sub>.” has been added in Lines 24-29  
7 Page 13 to Lines 1-4 Page 14 of the revised manuscript.

8 (c) It has been proposed that the concentration of sulfuric acid is even greater than that of  
9 water vapor in the atmosphere of Venus (*Science*, 1990, 249, 1273.; *Planet. Space Sci.*, 2006, 54,  
10 1352.; *Icarus*, 1994, 109, 58.; *Nat. Geosci.*, 2010, 3, 834.), which may lead to that the SO<sub>3</sub> +  
11 H<sub>2</sub>SO<sub>4</sub> reaction is probably favorable than the H<sub>2</sub>O-assisted hydrolysis of SO<sub>3</sub> in the Venus’  
12 atmosphere. To check whether the SO<sub>3</sub> + H<sub>2</sub>SO<sub>4</sub> reaction is more favorable than H<sub>2</sub>O-assisted  
13 hydrolysis of SO<sub>3</sub> or not in the Venus’ atmosphere, the rate ratio of  $v_{\text{DSA}}/v_{\text{SA}}$  listed in Eq. 4 has  
14 been calculated in Table 2. It can be seen from Table 2 that the rate ratio of  $v_{\text{DSA}}/v_{\text{SA}}$  is  $3.24 \times 10^8$ -  
15  $5.23 \times 10^{10}$  within the altitude range of 40-70 km in the Venus’ atmosphere, which indicates that  
16 the SO<sub>3</sub> + H<sub>2</sub>SO<sub>4</sub> reaction is significantly more favorable than the hydrolysis reaction of SO<sub>3</sub> +  
17 (H<sub>2</sub>O)<sub>2</sub> within the altitudes range of 40-70 km in the Venus’ atmosphere. Based on this, the  
18 sentence of “Notably, as the concentration of sulfuric acid was even greater than that of water  
19 vapor in the atmosphere of Venus, the SO<sub>3</sub> + SA reaction was probably favorable than the H<sub>2</sub>O-  
20 assisted hydrolysis of SO<sub>3</sub> in the Venus’ atmosphere. To check whether the SO<sub>3</sub> + H<sub>2</sub>SO<sub>4</sub> reaction  
21 was more favorable than H<sub>2</sub>O-assisted hydrolysis of SO<sub>3</sub> or not in the Venus’ atmosphere, the rate  
22 ratio of  $v_{\text{DSA}}/v_{\text{SA}}$  listed in Eq. 4 has been calculated in Table 2. It can be seen from Table 2 that the  
23 rate ratio of  $v_{\text{DSA}}/v_{\text{SA}}$  was  $3.24 \times 10^8$ - $5.23 \times 10^{10}$  within the altitude range of 40-70 km in the  
24 Venus’ atmosphere, which indicates that the SO<sub>3</sub> + H<sub>2</sub>SO<sub>4</sub> reaction is significantly more favorable  
25 than the hydrolysis reaction of SO<sub>3</sub> + (H<sub>2</sub>O)<sub>2</sub> within the altitudes range of 40-70 km in the Venus’  
26 atmosphere.” has been added in Lines 4-11 Page 14 of the revised manuscript.

27 Overall, it is important to study the mechanism between SO<sub>3</sub> and H<sub>2</sub>SO<sub>4</sub> and the competition  
28 between the SO<sub>3</sub> + H<sub>2</sub>SO<sub>4</sub> reaction and H<sub>2</sub>O-assisted hydrolysis. The SO<sub>3</sub> + SA reaction cannot  
29 compete with H<sub>2</sub>O-assisted hydrolysis of SO<sub>3</sub> within the altitude range of 0-30 km in the Earth’s  
30 atmosphere, even considering of high H<sub>2</sub>SO<sub>4</sub> concentration at the end and outside the aircraft

1 engine and flight. However, the  $\text{SO}_3 + \text{SA}$  reaction is significantly more favorable than the  
2 hydrolysis reaction of  $\text{SO}_3 + (\text{H}_2\text{O})_2$  within the altitude range of 40-70 km in the Venus'  
3 atmosphere.

4 **Comment 13.**

5 **Line 181:** *“Therefore, it can be said that the direct reaction between  $\text{SO}_3$  and SA is more  
6 favorable over  $\text{H}_2\text{O}$ -catalyzed hydrolysis of  $\text{SO}_3$  energetically and kinetically.”*

7 I believe this conclusion should be based on the “reaction rates” and not the “reaction rate  
8 constants”.

9 **Response:** Thank you for your valuable comments. We agree with the suggestion of the reviewer  
10 that the conclusion should be based on the “reaction rates” and not the “reaction rate constants”.  
11 So, in Lines 16-17 Page 8 of the revised manuscript, the sentence of “**Therefore, it can be said that  
12 the direct reaction between  $\text{SO}_3$  and SA is more favorable over  $\text{H}_2\text{O}$ -catalyzed hydrolysis of  $\text{SO}_3$   
13 energetically and kinetically.**” has been changed as “**Therefore, it can be said that the direct  
14 reaction between  $\text{SO}_3$  and SA occurs easily under atmospheric conditions.**”.

15

16 **Comment 14.1.**

17 **Section 3.2:** The first two sentences are contradicting each other. Is the mechanism lacking or  
18 does it have high reactivity? I am also missing some information about how the system was setup.

19 **Response:** Thanks for your valuable comments. According to suggestion of reviewers, the first  
20 two sentences in the section of “**3.2 Reactions at the Air-water interface**” has been re-organized.  
21 The mechanism for the  $\text{SO}_3 + \text{SA}$  reaction at the air-water interface was lacking and thus BOMD  
22 simulations were used to evaluate the reaction mechanism of  $\text{SO}_3$  with SA at the aqueous  
23 interfaces. This reaction on water surface may occur in three ways: (i)  $\text{SO}_3$  colliding with adsorbed  
24  $\text{H}_2\text{SO}_4$  at the air-water interface; (ii)  $\text{SO}_3$  colliding with adsorbed  $\text{SO}_3$  at the aqueous interface; or  
25 (iii) the  $\text{SO}_3\text{-H}_2\text{SO}_4$  complex reacting at the aqueous interface. However, due to the high reactivity  
26 both of  $\text{SO}_3$  and  $\text{H}_2\text{SO}_4$  with interfacial water, the lifetimes of  $\text{SO}_3$  and  $\text{H}_2\text{SO}_4$  on the water droplet  
27 are extremely short (on the order of a few picoseconds). Thus, two possible models were mainly  
28 considered for the  $\text{SO}_3 + \text{H}_2\text{SO}_4$  reaction on the water surface: (i) gaseous  $\text{SO}_3$  colliding with  
29  $\text{HSO}_4^-$  at the air-water interface and (ii) the DSA (the gas-phase product of  $\text{SO}_3$  and  $\text{H}_2\text{SO}_4$ )  
30 dissociating on water droplet. Based on this, the sentence of “**Similar with the interfacial reaction**

1 of SO<sub>3</sub> with organic and inorganic acids (Cheng et al., 2023; Zhong et al., 2016), the reaction  
2 between SO<sub>3</sub> and SA at the aqueous interface may occur in three ways: (i) SO<sub>3</sub> colliding with  
3 adsorbed SA at the air-water interface; (ii) SO<sub>3</sub> colliding with adsorbed SO<sub>3</sub> at the aqueous  
4 interface; or (iii) the SO<sub>3</sub>-SA complex reacting at the aqueous interface. However, due to the high  
5 reactivity both of SO<sub>3</sub> and SA at the air-water interface, the lifetimes of SO<sub>3</sub> (Zhong et al., 2019)  
6 and SA (Fig. S2) (on the order of a few picoseconds) on the water droplet were extremely short  
7 and can be formed SA<sup>-</sup> ion quickly. Besides, as the calculated result above, SO<sub>3</sub>···H<sub>2</sub>SO<sub>4</sub> complex  
8 can be generate DSA easily before it approaches the air-water interface.” has been deleted in Lines  
9 17-25 Page 10 of the revised manuscript.

10  
11 **Comment 14.2.**

12 Would the studied compounds (SO<sub>3</sub>, H<sub>2</sub>SO<sub>4</sub> and H<sub>2</sub>S<sub>2</sub>O<sub>7</sub>) actually be at the interface or would they  
13 be solvated in the water cluster?

14 **Response:** Thanks for your valuable comments. According to suggestion of reviewers, the time  
15 evolution of the position (z coordinate) of SO<sub>3</sub>, SA and DSA molecules is monitored so as to  
16 observe whether these molecules stay at the air-water interface or in the water phase. The pie chart  
17 with the occurrence percentages of SO<sub>3</sub>, SA and DSA at the air-water interface and in water phase  
18 has been displayed in Fig. S2. As seen in Fig. S2, the SO<sub>3</sub>, SA and DSA molecules can stay at the  
19 interface for 35.8%, 30.1% and 39.2% of the time in the 150 ns simulation (Fig. S2), respectively,  
20 revealing that the existence of SO<sub>3</sub>, SA and DSA at the air-water interface cannot be negligible.

21  
22 **Comment 14.3.**

23 Is the reaction an artefact of not equilibrating the system before setting up the reaction?

24 **Response:** Thanks for your valuable comments. The droplet system with 191 water molecules has  
25 been equilibrated before SO<sub>3</sub> and H<sub>2</sub>SO<sub>4</sub> was added at the water surface. Specifically, a nearly  
26 spherical droplet with 191 water molecules was firstly constructed by using the Packmol program  
27 (*J. Comput. Chem.*, 2009, 30, 2157-2164.) with a tolerance of 2.0 Å, namely, all atoms from  
28 different molecules will be at least 2.0 Å apart. Then, based on the resulting initial structure, the  
29 GROMACS software (*J. Comput. Chem.*, 2005, 26, 1701-1718.) with the general AMBER force  
30 field (GAFF) (*J. Comput. Chem.* 2004, 25, 1157-1174.) was used to simulate the droplet

1 equilibrium process with two steps. In the first step, a water slab of  $35 \times 35 \times 35 \text{ \AA}^3$  containing  
2 191 water molecules was built using periodic boundary conditions to avoid the effect of  
3 neighboring replicas. In the second step, the water slab was fully equilibrated for 1 ns under NVT  
4 ensemble (N, V and T represent the number of atoms, volume and temperature, respectively) to  
5 reach equilibrium state. The water molecules were described by the TIP3P model. The isothermal-  
6 isochoric (NVT) simulation was executed at 298 K for simulation system. The temperature was  
7 kept constant by the V-rescale thermostat coupling algorithm. The coupling time constant is 0.1 ps.  
8 Bond lengths were constrained by the LINCS algorithm. The cut-off distance of 1.2 nm was set  
9 for van der Waals (vdW) interactions. The Particle Mesh Ewald (PME) summation method was  
10 used to calculate the electrostatic interactions. During the whole simulation process, a time step of  
11 2 fs was set and three-dimensional periodic boundary conditions were adopted. Next, to ensure the  
12 stability of the system, the droplets were pre-optimized using BOMD at 300 K for 10 ps prior to  
13 the simulation of the air-water interfacial reaction. Using the density functional theory (DFT)  
14 method, the electronic exchange-correlation term was described by the Becke-Lee-Yang-Parr  
15 (BLYP) functional. The Grimme's dispersion correction (D3) was applied to account for the weak  
16 dispersion interaction. The double- $\zeta$  Gaussian (DZVP-MOLOPT) basis set and the Goedecker-  
17 Teter-Hutter (GTH) norm-conserving pseudopotentials were adopted to treat the valence and the  
18 core electrons, respectively. The planewave cutoff energy is set to 280 Ry, and that for the  
19 Gaussian basis set is 40 Ry. And the SCF convergence criterion is  $1.0\text{E-}5$  Hartree. All simulations  
20 were performed in NVT ensemble with Nose-Hoover thermostat controlling the temperature.  
21 Finally, the  $\text{SO}_3$  and  $\text{H}_2\text{SO}_4$  molecule was added at the water surface after the droplet system with  
22 191 water molecules was fully equilibrated. The details of the equilibrium process for the droplet  
23 system with 191 water molecules are shown in the *SI Appendix* Part 4. Meanwhile, the sentence of  
24 "It is pointed out that the droplet system with 191 water molecules has been equilibrated before  
25  $\text{SO}_3$  and  $\text{H}_2\text{SO}_4$  was added at the water surface. The details of the equilibrium process for the  
26 droplet system with 191 water molecules are shown in the *SI Appendix* Part 4." has been added in  
27 Lines 22-25 Page 6 of revised manuscript.

28

29 **Comment 14.4.**

1 How many trajectories were carried out? Are adequate statistics ensured or can this be considered  
2 a “rare event”.

3 **Response:** Thanks for your valuable comments. In the interfacial reactions of (i) gaseous SO<sub>3</sub>  
4 colliding with SA<sup>-</sup> at the air-water interface and (ii) the DSA (the gas-phase product of SO<sub>3</sub> and  
5 SA) dissociating on water droplet, sufficient statistical data are available in each reaction  
6 mechanism. It is noted that 40 BOMD simulations were carried out in the air-water interface  
7 reactions to eliminate the influence of the initial configuration on the simulation results of  
8 interfacial reaction. So, the additional BOMD trajectories and snapshots for H<sub>2</sub>O-induced the  
9 formation of S<sub>2</sub>O<sub>7</sub><sup>2-</sup>⋯H<sub>3</sub>O<sup>+</sup> ion pair, HSO<sub>4</sub><sup>-</sup> mediated the formation of HSO<sub>4</sub><sup>-</sup>⋯H<sub>3</sub>O<sup>+</sup> ion pair and  
10 the deprotonation of H<sub>2</sub>S<sub>2</sub>O<sub>7</sub> has been added in Fig. S4, Figs. S5-S6 and Fig. S7, respectively. Due  
11 to the similarity of the same type of interfacial reaction mechanism, we do not list all the BOMD  
12 trajectories and snapshots for H<sub>2</sub>O-induced the formation of S<sub>2</sub>O<sub>7</sub><sup>2-</sup>⋯H<sub>3</sub>O<sup>+</sup> ion pair, HSO<sub>4</sub><sup>-</sup>  
13 mediated the formation of HSO<sub>4</sub><sup>-</sup>⋯H<sub>3</sub>O<sup>+</sup> ion pair and the deprotonation of H<sub>2</sub>S<sub>2</sub>O<sub>7</sub>. However, in  
14 Fig. S4-Fig. S7, at least 4 BOMD trajectories and snapshots were included in each Figure. Besides,  
15 the sentence of “To eliminate the influence of the initial configuration on the simulation results of  
16 interfacial reaction, 40 BOMD simulations for the air-water interface reactions were carried out.”  
17 has been added in Lines 3-5 Page 7 of revised manuscript.

18

#### 19 **Comment 14.5.**

20 What was the starting geometries? At the transition state?

21 **Response:** Thanks for your valuable comments. It is noted that the interfacial starting geometries  
22 are not the transition state in the reaction of SO<sub>3</sub> with SA at the air-water interface. Specially, (a)  
23 in H<sub>2</sub>O-induced the formation of S<sub>2</sub>O<sub>7</sub><sup>2-</sup>⋯H<sub>3</sub>O<sup>+</sup> ion pair from the reaction of SO<sub>3</sub> with HSO<sub>4</sub><sup>-</sup> at the  
24 air-water interface illustrated in Fig. 2 and Fig. S4, the starting geometries is the gaseous SO<sub>3</sub>  
25 collision with the adsorbed SA<sup>-</sup>, where the bond length between S1 atom of SO<sub>3</sub> and O1 atom of  
26 HSO<sub>4</sub><sup>-</sup> is set within the range of 3.0-4.0 Å; (b) In the hydration reaction mechanism of SO<sub>3</sub>  
27 mediated by HSO<sub>4</sub><sup>-</sup> at the air water interface illustrated in Fig. 3, Fig. S5 and Fig. S6, the starting  
28 geometries is the gaseous SO<sub>3</sub> collision with the adsorbed SA<sup>-</sup>, where the bond length between O4  
29 atom of SO<sub>3</sub> and H3 atom of HSO<sub>4</sub><sup>-</sup> is set within the range of 2.5-3.5 Å; (c) In the deprotonation of  
30 H<sub>2</sub>S<sub>2</sub>O<sub>7</sub> at the air water interface illustrated in Fig. 4 and Fig. S7, the starting geometries is the

1 adsorbed DSA, where the distance between DSA and interfacial water molecule is set within the  
2 range of 3.0-4.0 Å.

3

4 **Comment 14.6.**

5 Was the  $\text{SO}_3+\text{H}_2\text{O}$  reaction observed in any of the trajectories? The reaction without SA should  
6 also be tested.

7 **Response:** Thanks for your valuable comments. The interfacial hydration mechanism of  $\text{SO}_3$   
8 without  $\text{H}_2\text{SO}_4$  has been reported previously by Lv et al. (*Atmos. Environ.*, 2020, 230, 117514.)  
9 where the  $\text{SO}_3$  can react rapidly with water molecules to form the ion pair of  $\text{HSO}_4^-$  and  $\text{H}_3\text{O}^+$  or  
10  $\text{H}_2\text{SO}_4$  within a few picoseconds. Three different reaction pathways, namely no loop-structure  
11 formation, loop-structure formation with proton transfer in the loop and loop-structure formation  
12 with proton transfer outside the loop, can be found from the results of BOMD simulations reported  
13 by Lv et al. (*Atmos. Environ.*, 2020, 230, 117514.). So, the interfacial hydration mechanism of  
14  $\text{SO}_3$  without  $\text{H}_2\text{SO}_4$  has not been restudied here. However, the hydration reaction mechanism of  
15  $\text{SO}_3$  at the air-water interface reported by Lv et al. (*Atmos. Environ.*, 2020, 230, 117514.) has  
16 been compared with the interfacial hydration mechanism of  $\text{SO}_3$  mediated by  $\text{HSO}_4^-$  reported in  
17 the present work.

18 The interfacial hydration mechanism of  $\text{SO}_3$  mediated by  $\text{HSO}_4^-$  were observed in the BOMD  
19 simulations illustrated in Fig. 3, Fig. S5 and Fig. S6. Specifically, both direct (loop-structure  
20 formation with proton transfer outside the loop, Fig. 3(a), Fig. S5 and Movie S2) and indirect (no  
21 loop-structure formation, Fig. 3(b), Fig. S6 and Movie S3) forming mechanisms were observed in  
22  $\text{HSO}_4^-$ -mediated formation of  $\text{HSO}_4^- \cdots \text{H}_3\text{O}^+$  ion pair. The loop-structure formation with proton  
23 transfer in the loop was not observed in the BOMD simulations. The direct  $\text{HSO}_4^-$ -mediated  
24 formation of  $\text{HSO}_4^- \cdots \text{H}_3\text{O}^+$  ion pair was a loop structure mechanism, which was consistent with  
25 gas phase hydrolysis of  $\text{SO}_3$  assisted by acidic catalysts of  $\text{HCOOH}$ ,  $\text{HNO}_3$ ,  $\text{H}_2\text{C}_2\text{O}_4$  and  $\text{H}_2\text{SO}_4$  in  
26 the previous works (Long et al., 2012; Long et al., 2013a; Torrent-Sucarrat et al., 2012; Lv et al.,  
27 2019) and the hydration reaction mechanism of  $\text{SO}_3$  at the air water interface (*Atmos. Environ.*,  
28 2020, 230, 117514.). During the direct formation route of  $\text{HSO}_4^- \cdots \text{H}_3\text{O}^+$  ion pair,  $\text{HSO}_4^-$  played as  
29 a spectator, while interfacial water molecules acted as both a reactant and a proton acceptor. The  
30 indirect forming process of  $\text{HSO}_4^- \cdots \text{H}_3\text{O}^+$  ion pair contained two steps: (i)  $\text{SO}_3$  hydration along



1 with H<sub>2</sub>SO<sub>4</sub> formation and (ii) H<sub>2</sub>SO<sub>4</sub> deprotonation. During the whole indirect forming process of  
2 HSO<sub>4</sub><sup>-</sup>···H<sub>3</sub>O<sup>+</sup> ion pair, HSO<sub>4</sub><sup>-</sup> played as protons donor and acceptor, and water molecules acted as  
3 hydration reactants and proton acceptors. The direct HSO<sub>4</sub><sup>-</sup>-mediated formation of HSO<sub>4</sub><sup>-</sup>···H<sub>3</sub>O<sup>+</sup>  
4 ion pair needs less time than the indirect forming process of HSO<sub>4</sub><sup>-</sup>···H<sub>3</sub>O<sup>+</sup> ion pair. This is  
5 consistent with the interfacial reactions of CH<sub>2</sub>OO + HNO<sub>3</sub> (*J. Am. Chem. Soc.*, 2018, 140, 14,  
6 4913-4921.) and the hydration of SO<sub>3</sub> (*Atmos. Environ.*, 2020, 230, 117514.) where the direct  
7 forming mechanism needs less time than indirect forming mechanism.

8 Based on the discussion above, the sentence of “As compared with the hydration reaction  
9 mechanism of SO<sub>3</sub> at the air-water interface reported by Lv et al. (Lv and Sun, 2020), the loop-  
10 structure formation with proton transfer in the loop was not observed in the direct mechanism of  
11 SA<sup>-</sup>-mediated formation of SA<sup>-</sup>···H<sub>3</sub>O<sup>+</sup> ion pair. This is probably because SA<sup>-</sup> ion is more difficult  
12 to give the proton.” has been added in Lines 25-28 Page 12 of the revised manuscript. Meanwhile,  
13 the sentence of “Compared with the direct mechanism of SA<sup>-</sup>-mediated formation of SA<sup>-</sup>···H<sub>3</sub>O<sup>+</sup>  
14 ion pair, the indirect forming process of HSO<sub>4</sub><sup>-</sup>···H<sub>3</sub>O<sup>+</sup> ion pair required more time. This was  
15 consistent with the interfacial reactions of CH<sub>2</sub>OO + HNO<sub>3</sub> (Kumar et al., 2018) and the hydration  
16 of SO<sub>3</sub> (Lv and Sun, 2020) where the direct forming mechanism needed less time than indirect  
17 forming mechanism.” has been added in Lines 15-19 Page 12 of the revised manuscript.

18

19 **Comment 15.**

20 **Section 3.3:** There is heavy referencing to the SI. Please also add the relevant data to the text. For  
21 instance, at line 303, how can the H<sub>2</sub>S<sub>2</sub>O<sub>7</sub> formation reaction matter if SO<sub>3</sub> + (H<sub>2</sub>O)<sub>2</sub> is the major  
22 sink?

23 **Response:** Thank you for your valuable comments. According to your suggestion, the importance  
24 of the SO<sub>3</sub> + H<sub>2</sub>SO<sub>4</sub> reaction has been discussed and the competition between the SO<sub>3</sub> + H<sub>2</sub>SO<sub>4</sub>  
25 reaction and H<sub>2</sub>O-assisted hydrolysis of SO<sub>3</sub> in the atmospheres of Earth and Venus have been  
26 discussed. Moreover, the relevant data listed in supporting information has been added to the  
27 manuscript. The corresponding revision has been respectively made as follows.

28 (a) Sulfur trioxide (SO<sub>3</sub>) is a major air pollutant and can be considered as the most  
29 important oxidation product of SO<sub>2</sub>. As an active atmospheric species, SO<sub>3</sub> can lead to the  
30 formations of acid rain and atmospheric aerosol and thus plays a well-documented role in regional

1 climate and human health. In the atmosphere, the hydrolysis of SO<sub>3</sub> to product H<sub>2</sub>SO<sub>4</sub> (SA) is the  
 2 most major loss route of SO<sub>3</sub>. As a complement to the loss of SO<sub>3</sub>, ammonolysis reaction of SO<sub>3</sub>  
 3 in polluted areas of NH<sub>3</sub> can form H<sub>2</sub>NSO<sub>3</sub>H, which not only can be competitive with the  
 4 formation of SA from the hydrolysis reaction of SO<sub>3</sub>, but also can enhance the formation rates of  
 5 sulfuric acid (SA)-dimethylamine (NH(CH<sub>3</sub>)<sub>2</sub>, DMA) clusters by about 2 times. Similarity, SO<sub>3</sub>  
 6 can also react with NH<sub>3</sub>, CH<sub>3</sub>OH, HNO<sub>3</sub>, HCl, organic acids (such as HCOOH), and both  
 7 processes can provide a mechanism for incorporating organic matter into aerosol particles. These  
 8 reactions between SO<sub>3</sub> and trace atmosphere species above provide some complementary routes to  
 9 the loss of SO<sub>3</sub> in locally polluted areas. However, the reaction mechanism between SO<sub>3</sub> and  
 10 H<sub>2</sub>SO<sub>4</sub> has yet to be fully understood. Previous studies have shown that the concentration of water  
 11 vapor decreases significantly with increasing altitude (*J. Phys. Chem. A*, 2013, 117, 10381-10396.;  
 12 *J. Am. Chem. Soc.*, 2021, 143, 8402-8413.), leading to longer atmospheric lifetimes of SO<sub>3</sub>. The  
 13 gas phase reaction of SO<sub>3</sub> with H<sub>2</sub>SO<sub>4</sub> may contribute significantly to the loss of SO<sub>3</sub> in dry areas  
 14 where [H<sub>2</sub>SO<sub>4</sub>] is relatively high (especially at lower temperatures) and at higher altitude. So, the  
 15 reaction mechanism between SO<sub>3</sub> and H<sub>2</sub>SO<sub>4</sub> has been studied here, and the competition between  
 16 the SO<sub>3</sub> + H<sub>2</sub>SO<sub>4</sub> reaction and H<sub>2</sub>O-assisted hydrolysis of SO<sub>3</sub> have been discussed. Based on this,  
 17 the sentence of “Previous studies have shown that the concentration of water vapor decreases  
 18 significantly with increasing altitude, leading to longer atmospheric lifetimes of SO<sub>3</sub>. The gas  
 19 phase reaction of SO<sub>3</sub> with H<sub>2</sub>SO<sub>4</sub> may contribute significantly to the loss of SO<sub>3</sub> in dry areas  
 20 where [H<sub>2</sub>SO<sub>4</sub>] is relatively high (especially at lower temperatures) and at higher altitude. So, it is  
 21 important to study the reaction mechanism of SO<sub>3</sub> with H<sub>2</sub>SO<sub>4</sub> and its competition with H<sub>2</sub>O-  
 22 assisted hydrolysis of SO<sub>3</sub>.” has been added in Lines 7-12 Page 3 of the revised manuscript.

23 (b) In the gas-phase, the main sink route of SO<sub>3</sub> is H<sub>2</sub>O-assisted hydrolysis of SO<sub>3</sub>. To  
 24 understand the competition between the SO<sub>3</sub> + H<sub>2</sub>SO<sub>4</sub> reaction and H<sub>2</sub>O-assisted hydrolysis of SO<sub>3</sub>  
 25 in the Earth’s atmosphere, the rate ratio (v<sub>DSA</sub>/v<sub>SA</sub>) between the SO<sub>3</sub> + H<sub>2</sub>SO<sub>4</sub> reaction and H<sub>2</sub>O-  
 26 assisted hydrolysis of SO<sub>3</sub> has been calculated and was expressed in Eq. (4).

$$27 \quad \frac{v_{\text{DSA}}}{v_{\text{SA}}} = \frac{k_{\text{DSA}} \times [\text{SO}_3] \times [\text{H}_2\text{SO}_4] + k_{\text{DSA\_WM}_s} \times K_{\text{eq1}} \times [\text{SO}_3] \times [\text{H}_2\text{SO}_4] \times [\text{H}_2\text{O}]}{k_{\text{SA\_WM}} \times K_{\text{eq2}} \times [\text{SO}_3] \times [\text{H}_2\text{O}] \times [\text{H}_2\text{O}]} \quad (4)$$

28 In Eq. (4), K<sub>eq1</sub> and K<sub>eq2</sub> were the equilibrium constant for the formation of H<sub>2</sub>SO<sub>4</sub>···H<sub>2</sub>O and  
 29 SO<sub>3</sub>···H<sub>2</sub>O complexes shown in Table S2, respectively; k<sub>DSA</sub>, k<sub>DSA\_WM\_s</sub> and k<sub>SA\_WM</sub> were

1 respectively denoted the bimolecular rate coefficient for the  $\text{H}_2\text{SO}_4 + \text{SO}_3$ ,  $\text{H}_2\text{SO}_4 \cdots \text{H}_2\text{O} + \text{SO}_3$   
2 and  $\text{SO}_3 \cdots \text{H}_2\text{O} + \text{H}_2\text{O}$  reactions;  $[\text{H}_2\text{O}]$  and  $[\text{H}_2\text{SO}_4]$  were respectively represented the  
3 concentration of  $\text{H}_2\text{O}$  and  $\text{H}_2\text{SO}_4$  taken from references (*J. Phys. Chem. A*, 2013, 117, 10381-  
4 10396.; *Environ. Sci. Technol.*, 2015, 49, 13112-13120.). The corresponding rate ratio have been  
5 listed in Table S7 (0 km altitude) and S8 (5-30 km altitude). As seen in Table S7, at 0 km altitude,  
6 the hydrolysis reaction of  $\text{SO}_3$  with  $(\text{H}_2\text{O})_2$  is more favorable than the  $\text{SO}_3 + \text{H}_2\text{SO}_4$  reaction as the  
7  $[\text{H}_2\text{O}]$  ( $10^{16}$ - $10^{18}$  molecules $\cdot\text{cm}^3$ ) is much larger than that of  $[\text{H}_2\text{SO}_4]$  ( $10^4$ - $10^8$  molecules $\cdot\text{cm}^3$ ).  
8 Although the concentration of water molecules decreases with the increase of altitude in Table S8,  
9 the concentration of  $[\text{H}_2\text{O}]$  is still much greater than that of  $[\text{H}_2\text{SO}_4]$ , resulting in the  $\text{SO}_3 + \text{H}_2\text{SO}_4$   
10 reaction cannot compete with  $\text{H}_2\text{O}$ -assisted hydrolysis of  $\text{SO}_3$  within the altitude range of 5-30 km.  
11 Moreover, the  $\text{SO}_3 + \text{H}_2\text{SO}_4$  reaction is not also the major sink route of  $\text{SO}_3$ , even considering of  
12 high  $\text{H}_2\text{SO}_4$  concentration at the end and outside the aircraft engine and flight. Based on this, the  
13 sentence of “The value of  $v_{\text{DSA}}/v_{\text{SA}}$  was listed in Table S7 (0 km altitude) and Table S8 (5-30 km  
14 altitude). As seen in Table S7, the hydrolysis reaction of  $\text{SO}_3$  with  $(\text{H}_2\text{O})_2$  is more favorable than  
15 the  $\text{SO}_3 + \text{H}_2\text{SO}_4$  reaction at 0 km altitude as the  $[\text{H}_2\text{O}]$  ( $10^{16}$ - $10^{18}$  molecules $\cdot\text{cm}^3$ ) is much larger  
16 than that of  $[\text{H}_2\text{SO}_4]$  ( $10^4$ - $10^8$  molecules $\cdot\text{cm}^3$ ). Although the concentration of water molecules  
17 decreases with the increase of altitude in Table S8, the concentration of  $[\text{H}_2\text{O}]$  is still much greater  
18 than that of  $[\text{H}_2\text{SO}_4]$ , resulting in the  $\text{SO}_3 + \text{H}_2\text{SO}_4$  reaction cannot compete with  $\text{H}_2\text{O}$ -assisted  
19 hydrolysis of  $\text{SO}_3$  within the altitude range of 5-30 km. Even considering of high  $\text{H}_2\text{SO}_4$   
20 concentration at the end and outside the aircraft engine and flight at 10 km (Curtius et al., 2002),  
21 the  $\text{SO}_3 + \text{H}_2\text{SO}_4$  reaction is not also the major sink route of  $\text{SO}_3$ .” has been added in Lines 24-29  
22 Page 13 to Lines 1-4 Page 14 of the revised manuscript.

23 (c) It has been proposed that the concentration of sulfuric acid is even greater than that of  
24 water vapor in the atmosphere of Venus (*Science*, 1990, 249, 1273.; *Planet. Space Sci.*, 2006, 54,  
25 1352.; *Icarus*, 1994, 109, 58.; *Nat. Geosci.*, 2010, 3, 834.), which may lead to that the  $\text{SO}_3 +$   
26  $\text{H}_2\text{SO}_4$  reaction is probably favorable than the  $\text{H}_2\text{O}$ -assisted hydrolysis of  $\text{SO}_3$  in the Venus’  
27 atmosphere. To check whether the  $\text{SO}_3 + \text{H}_2\text{SO}_4$  reaction is more favorable than  $\text{H}_2\text{O}$ -assisted  
28 hydrolysis of  $\text{SO}_3$  or not in the Venus’ atmosphere, the rate ratio of  $v_{\text{DSA}}/v_{\text{SA}}$  listed in Eq. 4 has  
29 been calculated in Table 2. It can be seen from Table 2 that the rate ratio of  $v_{\text{DSA}}/v_{\text{SA}}$  is  $3.24 \times 10^8$ -  
30  $5.23 \times 10^{10}$  in the 40-70 km altitude range of Venus, which indicates that the  $\text{SO}_3 + \text{H}_2\text{SO}_4$  reaction

1 is significantly more favorable than the hydrolysis reaction of  $\text{SO}_3 + (\text{H}_2\text{O})_2$  within the altitudes  
2 range of 40-70 km in the Venus' atmosphere. Based on this, the sentence of “Notably, as the  
3 concentration of sulfuric acid was even greater than that of water vapor in the atmosphere of  
4 Venus, the  $\text{SO}_3 + \text{SA}$  reaction was probably favorable than the  $\text{H}_2\text{O}$ -assisted hydrolysis of  $\text{SO}_3$  in  
5 the Venus' atmosphere. To check whether the  $\text{SO}_3 + \text{H}_2\text{SO}_4$  reaction was more favorable than  
6  $\text{H}_2\text{O}$ -assisted hydrolysis of  $\text{SO}_3$  or not in the Venus' atmosphere, the rate ratio of  $v_{\text{DSA}}/v_{\text{SA}}$  listed in  
7 Eq. 4 has been calculated in Table 2. It can be seen from Table 2 that the rate ratio of  $v_{\text{DSA}}/v_{\text{SA}}$  was  
8  $3.24 \times 10^8$ - $5.23 \times 10^{10}$  within the altitude range of 40-70 km in the Venus' atmosphere, which  
9 indicates that the  $\text{SO}_3 + \text{H}_2\text{SO}_4$  reaction is significantly more favorable than the hydrolysis  
10 reaction of  $\text{SO}_3 + (\text{H}_2\text{O})_2$  within the altitudes range of 40-70 km in the Venus' atmosphere.” has  
11 been added in Lines 4-11 Page 14 of the revised manuscript.

12 Overall, it is important to study the reaction mechanism of  $\text{SO}_3$  with  $\text{H}_2\text{SO}_4$  and its  
13 competition with  $\text{H}_2\text{O}$ -assisted hydrolysis of  $\text{SO}_3$ . The  $\text{SO}_3 + \text{SA}$  reaction cannot compete with  
14  $\text{H}_2\text{O}$ -assisted hydrolysis of  $\text{SO}_3$  within the altitude range of 0-30 km in the Earth's atmosphere,  
15 even considering of high  $\text{H}_2\text{SO}_4$  concentration at the end and outside the aircraft engine and flight.  
16 However, the  $\text{SO}_3 + \text{SA}$  reaction is significantly more favorable than the hydrolysis reaction of  
17  $\text{SO}_3 + (\text{H}_2\text{O})_2$  within the altitude range of 40-70 km in Venus' atmosphere.

18

19 **Comment 16.**

20 **Line 307-308:** The “stability analysis” should be added to the manuscript.

21 **Response:** Thank you for your valuable comments. According to your suggestion, the Gibbs free  
22 energy ( $\text{kcal}\cdot\text{mol}^{-1}$ ) diagram of  $(\text{DSA})_x(\text{SA})_y(\text{A})_z$  ( $z \leq x + y \leq 3$ ) clusters at 278.15K and 1 atm has  
23 been added in Fig. 5. Meanwhile, evaporation rate coefficient ( $\gamma$ ,  $\text{s}^{-1}$ ) for  $(\text{DSA})_x(\text{SA})_y(\text{A})_z$  ( $z \leq x +$   
24  $y \leq 3$ ) molecular clusters were calculated in Table S11-12. Based on this, the stability analysis  
25 for  $(\text{DSA})_x(\text{SA})_y(\text{A})_z$  ( $z \leq x + y \leq 3$ ) molecular clusters has been added in Lines 12-27 Page 14 of  
26 the revised manuscript, which has been organized as “From the multistep global minimum  
27 sampling technique, for  $(\text{DSA})_x(\text{SA})_y(\text{A})_z$  ( $z \leq x + y \leq 3$ ) molecular clusters, 27 most stable  
28 structures in the present system have been found (Fig. S11). To evaluate the thermodynamic  
29 stability of these clusters, Gibbs formation free energies ( $\Delta G$ ) at 278.15 K and evaporation rate  
30 coefficient ( $\gamma$ ,  $\text{s}^{-1}$ ) for  $(\text{DSA})_x(\text{SA})_y(\text{A})_z$  ( $z \leq x + y \leq 3$ ) molecular clusters were calculated in Fig.

1 5 and Table S11-12, respectively. As for dimers formed by SA, A and DSA, the  $\Delta G$  of  $(A)_1 \cdot$   
2  $(DSA)_1$  was  $-16.1 \text{ kcal}\cdot\text{mol}^{-1}$ , which was lowest in all dimers followed by  $(SA)_2$  ( $-8.5 \text{ kcal}\cdot\text{mol}^{-1}$ )  
3 and then  $(SA)_1 \cdot (A)_1$  ( $-6.3 \text{ kcal}\cdot\text{mol}^{-1}$ ), meanwhile, the  $\gamma$  of  $(A)_1 \cdot (DSA)_1$  ( $1.17 \times 10^{-3} \text{ s}^{-1}$ ) was  
4 lower than those of  $(SA)_2$  ( $3.81 \times 10^2 \text{ s}^{-1}$ ) and  $(SA)_1 \cdot (A)_1$  ( $4.19 \times 10^4 \text{ s}^{-1}$ ). Regarding for the SA-  
5 A-DSA-based clusters, the values of  $\Delta G$  and  $\gamma$  of SA-A-DSA-based clusters containing more DSA  
6 molecules were relatively lower than the corresponding values of other SA-A-DSA-based clusters  
7 with the same number of acid and base molecules. In the free-energy diagram for cluster  
8 formation steps of the SA-A-DSA system (Fig. 5), thermodynamic barriers were weakened mainly  
9 by the subsequential addition of A or DSA monomer. Also, the SA-A-DSA-based growth pathway  
10 was thermodynamically favorable with decreasing  $\Delta G$ . These results indicate that DSA not only  
11 can promote the stability of SA-A-DSA-based clusters but also may synergistically participate in  
12 the nucleation process.”

13  
14 **Comment 17.**

15 **Line 312:** The application of the enhancement factor yields an incorrect picture of the importance  
16 of  $\text{H}_2\text{S}_2\text{O}_7$  for cluster formation. Sulfuric acid and ammonia form very weakly bound electrically  
17 neutral clusters. Usually, ions are required to facilitate the process. Hence, large enhancement  
18 factors (R) are an artefact of dividing with a very small number. Please mention the absolute  
19 formation rates to ensure that the cluster formation rate is not zero.

20 **Response:** Thank you for your valuable comments. According to your suggestion, the formation  
21 rate of SA-A-DSA-based system has been mainly discussed rather than the enhancement factor.  
22 So, the influence of temperature and the precursor concentration on the formation rate ( $J, \text{cm}^{-3}\cdot\text{s}^{-1}$ )  
23 has been discussed and reorganized in the revised manuscript. The corresponding revision has  
24 been mainly made as follows.

25 (a) In Lines 28-30 Page 14 of the revised manuscript, the analysis of the influence of  
26 temperature on formation rate has been discussed and organized as “**The potential enhancement**  
27 **influence of DSA to the SA-A-based particle formation was shown in Fig. 6. The formation rate ( $J,$**   
28  **$\text{cm}^{-3}\cdot\text{s}^{-1}$ ) of SA-A-DSA-based system illustrated in Fig. 6 is negatively dependent on temperature,**  
29 **demonstrating that the low temperature is a key factor to accelerate cluster formation.”.**

1 (b) In Lines 4-6 Page 15 of the revised manuscript, the analysis of the influence of [DSA]  
2 has been discussed and organized as “In addition to temperature, the  $J$  of SA-A-DSA-based  
3 system shown in Fig. 6 rise with the increase of [DSA]. More notably, the participation of DSA  
4 can promote  $J$  to a higher level, indicating its enhancement on SA-A nucleation.”

5 (c) In Lines 6-13 Page 15 of the revised manuscript, the analysis of the influence of on both  
6 [SA] and [A] has been discussed and organized as “Besides, there was significantly positive  
7 dependence of the  $J$  of SA-A-DSA-based system on both [SA] and [A] in Fig. 7 (238.15 K) and  
8 Fig. S15-Fig. S18 (218.15, 258.15, 278.15 and 298.15 K). This was because the higher  
9 concentration of nucleation precursors could lead to higher  $J$ . Besides, Fig. S19 showed the  
10 nucleation rate when the sum ( $[SA] + [DSA]$ ) was kept constant.  $J_{DSA/SA}$  at substituted condition  
11 was higher than that at unsubstituted condition. These results indicated that DSA may can greatly  
12 enhance the SA-A particle nucleation in heavy sulfur oxide polluted atmospheric boundary layer,  
13 especially at an average flight altitude of 10 km with high [DSA].”

14  
15 **Comment 18.**

16 **Line 316:** An R value of 1.0 will mean that there is no enhancement. Hence, I do not believe that  
17 this can be stated. In addition, please add the numbers and explain how this conclusion of DSA  
18 being a “better enhancer” is drawn.

19 **Response:** Thank you for your valuable comments. We agree with the suggestion of the reviewer  
20 that it is incredible to use “enhancement factors” to explain the enhancing effect of the DSA.  
21 According to your suggestion, the formation rate of SA-A-DSA-based system has been mainly  
22 discussed rather than the enhancement factor. Meanwhile, the absolute formation rate has been  
23 used to explain why DSA promotes the nucleation of SA-A particles. The corresponding revision  
24 has been mainly made as follows.

25 (a) To evaluate the thermodynamic stability of these clusters, Gibbs formation free energies  
26 ( $\Delta G$ ) at 278.15 K and evaporation rate coefficient ( $\gamma$ ,  $s^{-1}$ ) for  $(DSA)_x(SA)_y(A)_z$  ( $z \leq x + y \leq 3$ )  
27 molecular clusters were calculated in Fig. 5 and Table S11-12, respectively. As for dimers formed  
28 by SA, A and DSA, the  $\Delta G$  of  $(A)_1 \cdot (DSA)_1$  is  $-16.1 \text{ kcal} \cdot \text{mol}^{-1}$ , which is lowest in all dimers  
29 followed by  $(SA)_2$  ( $-8.5 \text{ kcal} \cdot \text{mol}^{-1}$ ) and then  $(SA)_1 \cdot (A)_1$  ( $-6.3 \text{ kcal} \cdot \text{mol}^{-1}$ ), meanwhile, the  $\gamma$  of  
30  $(A)_1 \cdot (DSA)_1$  ( $1.17 \times 10^{-3} \text{ s}^{-1}$ ) is lower than those of  $(SA)_2$  ( $3.81 \times 10^2 \text{ s}^{-1}$ ) and  $(SA)_1 \cdot (A)_1$  ( $4.19 \times$

1  $10^4 \text{ s}^{-1}$ ). Regarding for the SA-A-DSA-based clusters, the values of  $\Delta G$  and  $\gamma$  of SA-A-DSA-based  
2 clusters containing more DSA molecules are relatively lower than the corresponding values of  
3 other SA-A-DSA-based clusters with the same number of acid and base molecules. In the free-  
4 energy diagram for cluster formation steps of the SA-A-DSA system (Fig. 5), thermodynamic  
5 barriers are weakened mainly by the subsequential addition of A or DSA monomer. Moreover, the  
6  $J$  of SA-A-DSA-based system shown in Fig. 6 rise with the increase of [DSA]. More notably, the  
7 participation of DSA can promote  $J$  to a higher level, indicating its enhancement on SA-A  
8 nucleation.

9 (b) The influence of temperature and the precursor concentration on the formation rate ( $J$ ,  
10  $\text{cm}^{-3}\cdot\text{s}^{-1}$ ) has been discussed in Lines 1-8 Page 15 of the revised manuscript. The detail  
11 information is also provided in **Comment 17**.

12 (c) The contribution of the DSA participation pathway has been increased with increasing  
13 temperature. Also, the contribution of the pathway with participation of DSA increases with  
14 increasing [DSA], while the number of DSA molecules contained in clusters [(SA)<sub>2</sub>·(A)<sub>3</sub>·DSA,  
15 SA·(A)<sub>2</sub>·DSA, SA·(A)<sub>3</sub>·(DSA)<sub>2</sub>, and (A)<sub>3</sub>·(DSA)<sub>3</sub>] that can contribute to cluster growth has a  
16 positive correlation with [DSA]. The corresponding revision has been made in Lines 20-24 Page  
17 15 of the revised manuscript.

18

19 **Comment 19.**

20 **Line 325:** Please mention the absolute rates here to let the reader know if this enhancement of  
21 many orders of magnitude is actually meaningful.

22 **Response:** Thank you for your valuable comments. According to your suggestion, the effects of  
23 precursor concentration and temperature are mainly described by the formation rate, meanwhile,  
24 the description of “enhancement factors” has been declined in the revised manuscript. The detail  
25 information is also provided in **Comment 17**.

26

27 **Comment 20.**

28 **Line 336-339:** *“Hence, it can be forecasted that the participation of DSA in SA-A-based NPF can  
29 likely enhance the number concentration of atmospheric particulates significantly in the polluted  
30 atmospheric boundary layer (278.15 K) areas with relatively high [DSA] and [A].”*

1 I do not believe this claim is adequately supported by the data. Please report the absolute values to  
2 support the conclusion.

3 **Response:** Thank you for your valuable comments. According to your suggestion, Meanwhile, the  
4 contribution of the DSA participation pathway has been increased with increasing temperature.  
5 Also, the contribution of the pathway with participation of DSA increases with increasing [DSA],  
6 while the number of DSA molecules contained in clusters [(SA)<sub>2</sub>·(A)<sub>3</sub>·DSA, SA·(A)<sub>2</sub>·DSA,  
7 SA·(A)<sub>3</sub>·(DSA)<sub>2</sub>, and (A)<sub>3</sub>·(DSA)<sub>3</sub>] that can contribute to cluster growth has a positive correlation  
8 with [DSA]. Based on this, the sentence of “Hence, it can be forecasted that the participation of  
9 DSA in SA-A-based NPF can likely enhance the number concentration of atmospheric particulates  
10 significantly in the polluted atmospheric boundary layer (278.15 K) areas with relatively high  
11 [DSA] and [A].” has been changed as “These results suggested that DSA has the ability to act as a  
12 potential contributor to SA-A-based NPF in the atmosphere at low *T*, low [SA], high [A] and high  
13 [DSA], and the DSA participation pathway can be dominant in heavy sulfur oxide polluted  
14 atmospheric boundary layer and in season of late autumn and early winter.”.

15

16 **Comment 21.**

17 **Line 367-368:** “Furthermore, the adsorption capacity of the S<sub>2</sub>O<sub>7</sub><sup>2-</sup>, H<sub>3</sub>O<sup>+</sup> and SA<sup>-</sup> to gaseous  
18 precursors in the atmosphere was further investigated.”

19 How was this evaluated? From Table 2 it looks like only the binding free energies were calculated.  
20 I guess the addition free energy of a given species should represent adsorption?

21 **Response:** Thanks for your valuable comments. Previous studies (*Angew. Chem. Int. Ed.*, 2019,  
22 131, 8439-8443.) have used the interaction free energies to assess the adsorption capacity of  
23 interfacial ions. So, we believe that it is reasonable to use the binding free energy to evaluate the  
24 adsorption capacity of the S<sub>2</sub>O<sub>7</sub><sup>2-</sup>, H<sub>3</sub>O<sup>+</sup> and SA<sup>-</sup> to gaseous precursors in the atmosphere. Our  
25 calculated the Gibbs free energies in Table 2 show that the interactions of S<sub>2</sub>O<sub>7</sub><sup>2-</sup>···H<sub>2</sub>SO<sub>4</sub>, S<sub>2</sub>O<sub>7</sub><sup>2-</sup>  
26 ···HNO<sub>3</sub>, S<sub>2</sub>O<sub>7</sub><sup>2-</sup>···(COOH)<sub>2</sub>, H<sub>3</sub>O<sup>+</sup>···NH<sub>3</sub>, H<sub>3</sub>O<sup>+</sup>···H<sub>2</sub>SO<sub>4</sub>, SA<sup>-</sup>···H<sub>2</sub>SO<sub>4</sub>, SA<sup>-</sup>···(COOH)<sub>2</sub>, and SA<sup>-</sup>  
27 ···HNO<sub>3</sub> are stronger than those of H<sub>2</sub>SO<sub>4</sub>···NH<sub>3</sub> (major precursor of atmospheric aerosols) with  
28 their binding free energies enhanced by 18.6-42.8 kcal·mol<sup>-1</sup>. These results reveal that interfacial  
29 S<sub>2</sub>O<sub>7</sub><sup>2-</sup>, SA<sup>-</sup> and H<sub>3</sub>O<sup>+</sup> can attract candidate species from the gas phase to the water surface.

30



1 **Comment 22.**

2 **Line 373-374:** I do not believe you can use a charged 2-3 molecular cluster in the gas-phase to  
3 draw conclusions about the “acceleration of particle growth”

4 **Response:** Thanks for your valuable comments. We agree with the suggestion of the reviewer that  
5 it is incorrect to use a charged 2-3 molecular cluster in the gas-phase to draw conclusions about  
6 the “acceleration of particle growth”. In Line 15 Page 16, of the revised manuscript “and thus in  
7 turn accelerates the growth of particle.” has been deleted; “enhancing potential of  $S_2O_7^{2-}$  on SA-A  
8 cluster” has been changed as “the nucleation potential of  $S_2O_7^{2-}$  on SA-A cluster” and In Lines 23-  
9 26 Page 16 of the revised manuscript “the Gibbs formation free energy  $\Delta G$  of  $(SA)_1(A)_1(S_2O_7^{2-})_1$   
10 cluster is lower. Therefore, we predict that  $S_2O_7^{2-}$  at the air-water interface has important  
11 implication to the aerosol NPF in highly industrial polluted regions with high concentrations of  
12  $SO_3$ .” has been changed as “the Gibbs formation free energy  $\Delta G$  of  $(SA)_1(A)_1(S_2O_7^{2-})_1$  cluster is  
13 lower, showing  $S_2O_7^{2-}$  ion at the air-water interface has stronger nucleation ability than  $X$  in the  
14 gas phase. Therefore, we predict that  $S_2O_7^{2-}$  at the air-water interface has stronger nucleation  
15 potential.”. The  $S_2O_7^{2-}$  ion at the air-water interface has stronger nucleation potential as the  
16 following reasons. One reason is that the interactions of  $S_2O_7^{2-} \cdots H_2SO_4$ ,  $S_2O_7^{2-} \cdots HNO_3$ ,  $S_2O_7^{2-}$   
17  $\cdots (COOH)_2$ ,  $H_3O^+ \cdots NH_3$ ,  $H_3O^+ \cdots H_2SO_4$ ,  $SA^- \cdots H_2SO_4$ ,  $SA^- \cdots (COOH)_2$ , and  $SA^- \cdots HNO_3$  listed  
18 in Table 2 are stronger than those of  $H_2SO_4 \cdots NH_3$  (major precursor of atmospheric aerosols).  
19 These results reveal that interfacial  $S_2O_7^{2-}$ ,  $SA^-$  and  $H_3O^+$  can attract candidate species from the  
20 gas phase to the water surface. The other reason is that as compared with  $(SA)_1(A)_1(X)_1$  ( $X =$   
21  $HOOCCH_2COOH$ ,  $HOCCOOSO_3H$ ,  $CH_3OSO_3H$ ,  $HOOCCH_2CH(NH_2)COOH$  and  $HOCH_2COOH$ )  
22 clusters (Zhong et al., 2019; Zhang et al., 2018; Rong et al., 2020; Gao et al., 2023; Liu et al.,  
23 2021a; Zhang et al., 2017), the number of hydrogen bonds in  $(SA)_1(A)_1(S_2O_7^{2-})_1$  cluster presented  
24 in Fig. S8 increased and the ring of the complex was enlarged. Meanwhile, comparing to  
25  $(SA)_1(A)_1(X)_1$  ( $X = HOOCCH_2COOH$ ,  $HOCCOOSO_3H$ ,  $CH_3OSO_3H$ ,  $HOOCCH_2CH(NH_2)COOH$   
26 and  $HOCH_2COOH$ ) clusters (Table 2), the Gibbs formation free energy  $\Delta G$  of  $(SA)_1(A)_1(S_2O_7^{2-})_1$   
27 cluster is lower, showing  $S_2O_7^{2-}$  ion at the air-water interface has stronger nucleation ability than  $X$   
28 in the gas phase.

29

30 **Comment 23.**

1 **Line 380-382:** “It was demonstrated that  $S_2O_7^{2-}$  has the highest potential to stabilize SA-A  
2 clusters and promote SA-A nucleation in these clusters due to its acidity and structural factors  
3 such as more intermolecular hydrogen bond binding sites”

4 I do not understand how this conclusion is drawn. What is the acidity of each of the compounds?

5 **Response:** Thanks for your valuable comments. The  $S_2O_7^{2-}$  ion is formed by two deprotonations  
6 of  $H_2S_2O_7$ , where the  $pK_{a1}$  and  $pK_{a2}$  of  $H_2S_2O_7$  are -16.05 and -4.81 (*Dalton Trans.*, 2013, 42,  
7 5566), respectively. This indicates that  $S_2O_7^{2-}$  is a strong acid anion. Moreover,  $S_2O_7^{2-}$  ion has  
8 many exposed O atoms, which suggests that  $S_2O_7^{2-}$  ion has more intermolecular hydrogen bond  
9 binding sites. Besides, the  $pK_a$  for X (X =  $HOOCCH_2COOH$ ,  $HOCCOOSO_3H$ ,  $CH_3OSO_3H$ ,  
10  $HOOCCH_2CH(NH_2)COOH$  and  $HOCH_2COOH$ ) has been listed in the Table S8.

11 Table S8 The  $pK_a$  for  $HOOCCH_2COOH$ ,  $HOCCOOSO_3H$ ,  $CH_3OSO_3H$ ,  
12  $HOOCCH_2CH(NH_2)COOH$  and  $HOCH_2COOH$

| Compound                            | $pK_{a1}$ | $pK_{a2}$ |
|-------------------------------------|-----------|-----------|
| $HOOCCH_2COOH$ <sup>a</sup>         | 2.85      | 5.89      |
| $HOCCOOSO_3H$ <sup>b</sup>          | 4.73      | -         |
| $CH_3OSO_3H$ <sup>c</sup>           | 10.2      | -         |
| $HOOCCH_2CH(NH_2)COOH$ <sup>d</sup> | 1.99      | 3.90      |
| $HOCH_2COOH$ <sup>e</sup>           | 3.83      | -         |

13 <sup>a</sup> The value was taken from reference (*J. Am. Chem. Soc.*, 1994, 116, 10298-10299.)

14 <sup>b and c</sup> The values were calculated at the M06-2X/6-311++G(3df,2pd) level.

15 <sup>d</sup> The value was taken from reference (Data for Biochemical Research, second ed., Oxford University Press,  
16 Oxford, 1969)

17 <sup>e</sup> The value was taken from reference (*Tissue Eng.*, 2007, 13, 2515-2523.)

18

19 **Comment 24.**

20 **Line 384:** An ion at a particle interface does not influence NPF.

21 **Response:** Thanks for your valuable comments. We agree with the suggestion of the reviewer that  
22 an ion at air-water interface is not directly related to new particle formation. Although the reaction  
23 of  $H_2S_2O_7$  or  $H_2SO_4$  formations at air-water interface is not directly related to new particle  
24 formation. In Line 15 Page 14, of the revised manuscript “and thus in turn accelerates the growth  
25 of particle.” has been deleted; “enhancing potential of  $S_2O_7^{2-}$  on SA-A cluster” has been changed  
26 as “the nucleation potential of  $S_2O_7^{2-}$  on SA-A cluster” and In Lines 23-26 Page 16 of the revised  
27 manuscript “the Gibbs formation free energy  $\Delta G$  of  $(SA)_1(A)_1(S_2O_7^{2-})_1$  cluster is lower. Therefore,

1 we predict that  $S_2O_7^{2-}$  at the air-water interface has important implication to the aerosol NPF in  
2 highly industrial polluted regions with high concentrations of  $SO_3$ .” has been changed as “the  
3 Gibbs formation free energy  $\Delta G$  of  $(SA)_1(A)_1(S_2O_7^{2-})_1$  cluster was lower, showing  $S_2O_7^{2-}$  ion at  
4 the air-water interface has stronger nucleation ability than  $X$  in the gas phase. Therefore, we  
5 predict that  $S_2O_7^{2-}$  at the air-water interface has stronger nucleation potential.”. The  $S_2O_7^{2-}$  ion at  
6 the air-water interface has stronger nucleation potential as the following reasons. One reason is  
7 that the interactions of  $S_2O_7^{2-}\cdots H_2SO_4$ ,  $S_2O_7^{2-}\cdots HNO_3$ ,  $S_2O_7^{2-}\cdots (COOH)_2$ ,  $H_3O^+\cdots NH_3$ ,  
8  $H_3O^+\cdots H_2SO_4$ ,  $SA^-\cdots H_2SO_4$ ,  $SA^-\cdots (COOH)_2$ , and  $SA^-\cdots HNO_3$  listed in Table 2 are stronger than  
9 those of  $H_2SO_4\cdots NH_3$  (major precursor of atmospheric aerosols). These results reveal that  
10 interfacial  $S_2O_7^{2-}$ ,  $SA^-$  and  $H_3O^+$  can attract candidate species from the gas phase to the water  
11 surface. The other reason is that as compared with  $(SA)_1(A)_1(X)_1$  ( $X = HOOCCH_2COOH$ ,  
12  $HOCCOOSO_3H$ ,  $CH_3OSO_3H$ ,  $HOOCCH_2CH(NH_2)COOH$  and  $HOCH_2COOH$ ) clusters (Zhong et  
13 al., 2019; Zhang et al., 2018; Rong et al., 2020; Gao et al., 2023; Liu et al., 2021a; Zhang et al.,  
14 2017), the number of hydrogen bonds in  $(SA)_1(A)_1(S_2O_7^{2-})_1$  cluster presented in Fig. S8 increased  
15 and the ring of the complex was enlarged. Meanwhile, comparing to  $(SA)_1(A)_1(X)_1$  ( $X =$   
16  $HOOCCH_2COOH$ ,  $HOCCOOSO_3H$ ,  $CH_3OSO_3H$ ,  $HOOCCH_2CH(NH_2)COOH$  and  $HOCH_2COOH$ )  
17 clusters (Table 2), the Gibbs formation free energy  $\Delta G$  of  $(SA)_1(A)_1(S_2O_7^{2-})_1$  cluster is lower,  
18 showing  $S_2O_7^{2-}$  ion at the air-water interface has stronger nucleation ability than  $X$  in the gas phase.  
19